BBA - Molecular Cell Research 1871 (2024) 119647

Contents lists available at ScienceDirect

BBA - Molecular Cell Research

journal homepage: www.elsevier.com/locate/bbamcr

Research paper

The dynamics of the electrotactic reaction of mouse 3T3 fibroblasts

Slawomir Lasota *, Eliza Zimolag, Sylwia Bobis-Wozowicz, Jagoda Pilipiuk, Zbigniew Madeja *

Jagiellonian University, Faculty of Biochemistry, Biophysics and Biotechnology, Department of Cell Biology, Gronostajowa 7, 30–387 Kraków, Poland

ARTICLE INFO

Keywords:
Electrotaxis
Electric field
Directional movement
Dynamics
Ion channels
Fibroblasts

ABSTRACT

The molecular mechanisms behind electrotaxis remain largely unknown, with no identified primary direct current electric field (dcEF) sensor. Two leading hypotheses propose mechanisms involving the redistribution of charged components in the cell membrane (driven by electrophoresis or electroosmosis) and the asymmetric activation of ion channels. To investigate these mechanisms, we studied the dynamics of electrotactic behaviour of mouse 3T3 fibroblasts.

We observed that 3T3 fibroblasts exhibit cathodal migration within just 1 min when exposed to physiological dcEF. This rapid response suggests the involvement of ion channels in the cell membrane. Our large-scale screening method identified several ion channel genes as potential key players, including the inwardly rectifying potassium channel Kir4.2. Blocking the Kir channel family with Ba^{2+} or silencing the Kcnj15 gene, encoding Kir4.2, significantly reduced the directional migration of 3T3 cells. Additionally, the levels of the intracellular regulators of Kir channels, spermine (SPM) and spermidine (SPD), had a significant impact on cell directionality. Interestingly, inhibiting Kir4.2 resulted in the temporary cessation of electrotaxis for approximately 1–2 h before its return. This observation suggests a two-phase mechanism for the electrotaxis of mouse 3T3 fibroblasts, where ion channel activation triggers the initial rapid response to dcEF, and the subsequent redistribution of membrane receptors sustains long-term directional movement.

In summary, our study unveils the involvement of Kir channels and proposes a biphasic mechanism to explain the electrotactic behaviour of mouse 3T3 fibroblasts, shedding light on the molecular underpinnings of electrotaxis.

1. Introduction

Directional cell migration is a complex process that plays a key role in several physiological events and many diseases. The most well-known mechanism that affects the direction of cell movement is chemotaxis [1–4]. However, directional cell migration is induced not only by chemoattractants but also by physical cues such as substrate anisotropy (contact guidance) or electric fields (electrotaxis) [5–8]. Electrotaxis is defined as an active directional movement towards the cathode or anode and is a major cellular effect of direct-current electric fields (dcEFs). The presence of endogenous electric fields in various localizations in living organisms has been described in many reports (for a review see McCaig et al. [9]). Such electric fields are formed as a result of the polarized transport of ions across the epithelium, which leads to the creation of a transepithelial potential. After rupture of the epithelium (for example, as a result of an injury), the TEP collapses at the wound centre but remains stable distally, at the place where ion transport is unaffected. The resulting voltage gradient establishes the dcEF with a vector parallel to the epithelial surface and the wound centre as the cathode [10]. The presence of such steady currents and dcEFs has been detected in the case of amputated amphibian limbs and human finger tips, corneal and ocular lens epithelial wounds and skin wounds, damaged bone, and transected sites of the spinal cord [11–13]. Accumulating evidence suggests that electric signals have an important role in directing cell migration in wound healing, embryonic development, and cancer metastasis [7,9,14]. Interestingly, although electrotaxis clearly overrides other directional signals involved in the regulation of cell migration, it has not attracted enough attention from researchers [14].

Although the phenomenon of electrotaxis has been well documented for a variety of cells, the molecular mechanisms used by cells to detect electric fields are largely unknown. Furthermore, no single electrotaxis sensor has been identified. Because of the high resistance of the cellular plasma membrane compared to that of the external media, searches for a sensor of the electric field of electrotaxing cells are focused on the cell

* Corresponding authors.
E-mail addresses: slawomir.lasota@uj.edu.pl (S. Lasota), z.madeja@uj.edu.pl (Z. Madeja).

https://doi.org/10.1016/j.bbamcr.2023.119647
Received 6 October 2023; Received in revised form 22 November 2023; Accepted 5 December 2023
Available online 11 December 2023

membrane. A plausible hypothesis assumes that electrostatic or electroosmotic forces redistribute charged components of the cell membrane, including receptors for chemoattractants. The increase in the density of membrane receptors on the cathode (or anode) facing side of the cell would be responsible for asymmetric signalling and directional motility. In this model, the molecular mechanism of induction of directional movement is the same in electrotaxis and chemotaxis (i.e., asymmetric activation of receptors of chemoattractants); however, in chemotaxis, it is caused by a gradient of chemoattractants, while in electrotaxis, it is caused by redistribution (accumulation at one side of cell) of the receptors for chemoattractants [9,15]. This mechanism elegantly adapts the molecular mechanisms of chemotaxis to explain the electrotactic reaction mechanisms. However, because the electrotactic reaction was also observed without any exogenous chemoattractants (for example, in serum-free media), it is not clear how those receptors are activated in this case. It is suggested that the mechanism responsible for this effect may be the clustering of receptors and activation of signalling in a ligand-independent manner or autocrine secretion of ligands [1]. Moreover, the mechanism of receptor translocation does not sufficiently explain the nature of the first, very fast reactions of cells to dcEF [6,7]. The mechanism of receptor translocation adopted an original concept of Jaffe [16] proposed for the explanation of the effect of dcEF on the growth and functional polarization of plant and animal tissues, which was limited to the action of sufficiently long-lasting dcEF. This model was restricted to a time range of approximately 10^4 s, that is, approximately 3 h, for a 30 μm diameter cell. Although subsequent studies [17,18] have shown that the redistribution of receptors can occur much faster, this time seems too long to explain the first observed signs of a cell's response to the electric field.

The second important hypothesis suggests that the electrotactic mechanism may be based on the asymmetrical activation of various ion channels of the cell membrane. Asymmetrical activation of ion channels by external dcEFs would be caused by hyperpolarization of the cell membrane at the anodal side and depolarization at the cathodal side of the cell. These changes would, in turn, affect the opening probability of voltage-gated ion channels (on the cathodal side of a cell) as well as create an asymmetric electromotive force for ionic flow once other ion channels are open (at the anodal side of a cell) [15,19,20]. The other suggested mechanism of activation of ion channels is that electrostatic and/or electroosmotic forces at the plasma membrane would apply a mechanical force on the cell and activate tension-sensitive cell surface components, such as stretch-activated ion channels [15]. These mechanisms (i.e., activation of ion channels) explain several observations, such as, for example, a very fast initial reaction of some cells to electric fields [6,7,21,22], the role of extracellular Ca^{2+} influx in efficient electrotaxis and the involvement of several types of ion channels in the electrotactic response [23–25]. In fact, both mechanisms (ion channel activation or receptor redistribution) are not mutually exclusive and may play a complementary role in electrotactic migration. However, the primary mechanism is still unknown. It seems that in the search for the overriding mechanism of electrotaxis, and therefore also the primary sensor of the electric field, an important element is the dynamics of the cell's reaction to the electric field.

In our previous paper [6], we demonstrated that in the case of *Amoeba proteus* (an extremely fast-moving unicellular organism), primary cell responses occurred <1 s after reversal of dcEF polarity. We also observed a very fast cell reaction (approximately 30 s) in several types of tissue cells [7,21,22]. These results were difficult to reconcile with hypotheses that try to explain cell electrotaxis only as a result of membrane protein lateral electrophoresis or electroosmosis. On the other hand, observations that the time needed for a clear accumulation of receptors on one side of the cell is approximately 10 min indicate that electromigration of surface macromolecules precedes or occurs at the same time as significant changes in directed migration of tissue cells [18]. It should be noted that in these experiments, the dynamics of the cell reaction to dcEFs were estimated by changes in the centroid position of the cell. However, measurements of the dynamics of cell reactions for dcEF by analysis of extending and retracting cell regions (facing cathode or anode) revealed that the primary reaction of the cell for electric field is much faster [6]. Our previous research was conducted primarily using very fast migrating cells such as *Amoeba proteus* and rat Walker carcinosarcoma cells (WC 256) [6,21]. For this reason, in the present report, we verify whether such a fast electrotactic reaction is also characteristic of very slowly migrating mouse 3T3 fibroblasts. For this purpose, we constructed an experimental model that enables investigations of the dynamics of electrotactic reactions of slowly migrating cells and the performance of a quantitative analysis of the reaction by analysis of morphological changes observed at the cathodal and anodal side of a cell migrating in dcEF. The results obtained confirmed that 3T3 fibroblasts migrate cathodally at electrical fields of physiological strength (1 V/cm). We observed an immediate response of cells to dcEF, with the first symptoms visible after 1 min of exposure to dcEF. The mechanism that is more likely to be involved in such a fast response of fibroblasts to dcEF could involve the opening of membrane ion channels. A large-scale screening method that we used to identify ion channel genes that are important in 3T3 electrotaxis revealed that several ion channel genes may be involved in this process. Among others, we observed that it strongly depends on inwardly rectifying potassium channels (Kir4.2), which were suggested to be involved in the electrotaxis of epithelial cells [26].

The obtained results indicate that the electrotaxis mechanism based on the activation of ion channels is probably not related to the activation of one type of channel but is a more complex phenomenon in which many types of ion channels may participate. Moreover, our data suggest a biphasic mechanism of electrotaxis of mouse 3T3 fibroblasts, in which the activation of ion channels is responsible for the first quick reaction of the cell to an electric field and the redistribution of membrane receptors for long-term maintenance of the direction of cell movement.

2. Materials and methods

2.1. Cell culture

Mouse 3T3 fibroblasts (Clontech, Cat. No. 630914, and ATCC CRL-1658) were cultured in DMEM HG (Dulbecco's modified Eagle's Medium High Glucose) medium (Sigma–Aldrich, St. Louis, MO, USA) supplemented with 10 % FBS (Foetal Bovine Serum) (Gibco, Waltham, MA, USA), penicillin (100 I.U./ml) and streptomycin (100 μg/ml) (referred to as 'complete culture medium') under standard conditions of 37 °C and 5 % CO_2. Cells were passaged with 0.25 % trypsin/EDTA (Gibco, Waltham, MA, USA) approximately every third day to ensure confluency that remained below 80 %.

2.2. Application of electric field

To apply a direct current electric field (dcEF) to the cells, we utilized a custom-made electrotactic chamber following a previously described protocol with minor adjustments [27]. Specifically, a total of 1×10^4 cells were seeded onto the centre of a sterile cover glass measuring 60 × 35 × 0.2 mm using 400 μl of complete culture medium, resulting in a final cell density of approximately 2.5×10^3 cells/cm^2. Immediately before the experiment, the second part of the observation chamber was assembled using another cover glass and two additional glass pieces measuring 60 × 10 × 0.2 mm, all connected with double-sided adhesive tape (tesa SE, Hamburg, Germany). During the chamber assembly process, both parts were connected and filled with fresh complete culture medium and then placed within an external electrotactic chamber constructed of PVC. Ag|AgCl electrodes (each with an area of 6 cm^2) were immersed in PBS and connected to a power supply. These electrodes were connected to the observation chamber using salt bridges made of glass pipes filled with agar (2 % in 0.5 M KCl). A direct current electric field with a specified intensity range of 0.5–4 V/cm was applied.

To ensure constant monitoring of the dcEF intensity, measuring electrodes were placed at the edges of the observation chamber.

2.3. Time-lapse imaging

Cell migration was monitored using a Leica DM IL LED microscope (Leica, Wetzlar, Germany) equipped with a CMOS Moticam 3 digital camera, which was controlled by Motic Image Plus 2.0 software (both from Motic, Xiamen, China). The microscope was equipped with either a 10× or 20× objective lens and a custom-made heating chamber to maintain a temperature of 37 °C near the observed cells. Images were acquired using integrated modulation contrast (IMC). To compensate for the absence of CO_2 control, HEPES buffer (15 mM) was added to the complete culture medium before each recording session.

The application of dcEF occurred after the initial 30 min to establish stable recording conditions. The negative electrode (cathode) was consistently placed on the right side of the field of view, and when necessary, it was occasionally replaced with the anode. The resulting image series were routinely aligned using Fiji ImageJ 1.51n software (National Institutes of Health, Bethesda, MD, USA) [28] to correct for image drift.

2.4. Analysis of single-cell migration

Cell migration was analysed as described previously using Hiro 1.0.0.4v software, developed by W. Czapla in Krakow, Poland [21,27,29]. Manual selection of cell centroids was performed on images taken at intervals of either 30 s or 5 min, depending on the specific experiment. The designated points were then connected using the software to generate cell migration trajectories, which were subsequently used to calculate various quantitative parameters:

- Speed of cell migration – determined by dividing the total length of the cell trajectory by the duration of the recording;
- Displacement – refers to the line connecting the initial and final points of the cell trajectory;
- CME (Coefficient of Movement Efficiency) – calculated as the quotient of displacement and the total length of the cell trajectory. It approaches 1 when cell migration is persistent and decreases towards 0 when the direction of movement changes frequently;
- Average directional cosine γ – calculated based on the angle (γ) between the dcEF vector and a line segment connecting the initial position with each subsequent position along the cell trajectory.

2.5. Analysis of electrotaxis dynamics

For electrotaxis dynamics analysis, time-lapse imaging was performed using a 30-s interval, consistent with previous procedures. However, in cases where migration reversal was an additional focus of analysis, a different approach was taken. After 2 h of continuous direct current electric field (dcEF) application with the cathode positioned on the right side, the dcEF direction was reversed by replacing the electrodes and transferring the cathode to the left side. Directional cosine γ values were then assigned for subsequent time intervals.

Detailed visualization of the response dynamics was achieved by manually outlining cell boundaries in microscopy images. The differences between the cell outlines at successive time intervals were evaluated, with newly covered areas highlighted in green, while areas released due to cell retraction are marked in red [22,27]. Quantitative analysis based on these cell regions was performed using Fiji ImageJ 1.51n [28]. A custom-made macro divided each outlined cell into three regions based on the axis parallel to the dcEF lines, resulting in three equal regions: right, left, and central (which was withdrawn). This division was performed at the moment of application or reversal of the dcEF, depending on the specific analysis. The areas of the right and left regions were measured and plotted to evaluate changes in cells facing the cathode and anode during response to dcEF application and reversal.

2.6. Pharmacological modification of signalling pathways

2.6.1. Calcium signalling

To investigate the role of calcium ions in the electrotaxis of 3T3 fibroblasts, we used various methods. This included conducting experiments in serum-free DMEM/F12 culture medium w/o calcium ions (Sigma–Aldrich) or the addition of EGTA (3 mM; Sigma–Aldrich) to complete culture medium (applied 30 min before and present in the course of the experiment) to remove extracellular Ca^{2+}. We also achieved intracellular calcium depletion by preincubating cells with BAPTA-AM (5 μM; Sigma–Aldrich) in serum-free culture medium for 30 min, followed by washing; BAPTA-AM was absent during the recording. For comprehensive calcium removal, we combined the use of EGTA and BAPTA-AM to eliminate both intra- and extracellular calcium. Furthermore, we inhibited voltage-gated calcium channels (VGCC) using verapamil (50 μM) and myosin light chain kinase (MLCK) with ML-7 (10 μM) (both Sigma–Aldrich). These inhibitors were introduced during chamber assembly and remained throughout the experiment.

2.6.2. EGFR signalling

To inhibit the EGF receptor and PI3K, we added AG1478 (3 μM) and LY-294002 (50 μM) (both Sigma–Aldrich), respectively, to the complete culture medium during chamber assembly. These inhibitors were introduced at least 30 min before recording cell migration and remained present throughout the experiment.

2.6.3. Kir channels activity

To modulate the activity of Kir channels, we used pharmacological inhibition with barium chloride ($BaCl_2$) (100–500 μM), which was added to the complete culture medium before recording and remained present during the experiment. We also manipulated the regulation of the Kir channels by modifying intracellular polyamine levels. Specifically, 3T3 fibroblasts were preincubated with DENSPM (the N1,N11-diethylnorspermine tetrahydrochloride) (25 μM; Tocris) for 48 h before the experiment. DENSPM activates SSAT (spermidine/spermine N1-acetyltransferase), leading to the acetylation of SPM/SPD polyamines and their depletion. Alternatively, we increased SPM/SPD polyamine levels by preincubating cells with putrescine (100 μM; Sigma–Aldrich) for 48 h, a precursor for their synthesis. We also modified Kir channel activity by elevating the intracellular Mg^{2+} ion concentration, achieved by adding $MgCl_2$ (10 mM) to the complete culture medium. This agent was consistently present throughout the recording session.

2.7. Cytometric analysis

To confirm the elevation of the level of intracellular magnesium ions after their external addition, 1×10^5 cells in suspension were loaded with mag-fluo-4AM (3 μM; ThermoFisher Scientific) for 20 min at 37 °C. Subsequently, they were washed three times with PBS and suspended in DMEM FluoroBrite culture medium (Gibco) containing 2 % FBS, with or without the addition of $MgCl_2$ (10 mM). Cytometric analysis was performed using an LSRFortessa flow cytometer (Becton Dickinson) to measure the increase in the green fluorescence of the cells. The acquired data were analysed with Flowing Software 2.5.1 and presented in the form of a histogram.

2.8. Knockdown of the Kcnj15 (Kir4.2) gene

Lentiviral vectors silencing the mouse Kcnj15 gene and coexpressing the GFP marker gene were produced in the HEK293T/17 (ATCC) packaging cell line by triple transfection with pLenti-Kcnj15-siRNA-GFP lentivector (ABM, Cat. No. i033064) and the packing plasmids psPAX2 and pMD2G (Addgene, #12260 and #12259, respectively) using

Lipofectamine 2000 according to the protocol provided by the producer. Control vectors, coding nontargeting shRNA or GFP only, were prepared with pLKO1-shRNA-nontargeting plasmid (Sigma–Aldrich) and the pEGIP plasmid (Addgene #26777) in the same way. Viral titres were determined using the same cell line. 3T3 fibroblasts were transduced with infectious viral particles at a multiplicity of infection of 15 in DMEM with low glucose supplemented with 1 % FBS and polybrene (10 μg/ml). Cells were transduced by centrifugation at 800 ×*g* for 30 min at 32 °C, after which FBS was added to the medium to a final concentration of 10 %. Cells were incubated with viral vectors overnight at 37 °C. Subsequently, the medium was replaced with standard cell culture medium. To obtain stably transduced cell lines, 3T3 cells were subjected to antibiotic selection using 10 μg/ml puromycin, which resistance gene was present in the introduced vectors. Selection was carried out for 2 days, and the presence of only GFP-positive cells was confirmed using fluorescence microscopy.

2.9. Western blot analysis

For each experimental condition, 1×10^6 cells were collected from the culture dish and lysed following a previously established protocol [30]. Protein levels were quantified using the Bradford method and compared to a BSA calibration curve. An SDS-polyacrylamide gel was prepared according to standard procedures [30]. Lysate samples containing 50 μg of protein, along with loading buffer and a protein marker, were loaded into gel wells. After electrophoresis, the proteins were transferred to a nitrocellulose membrane, which was later washed and blocked with 5 % skim milk in TBST. The membrane was then incubated overnight at 4 °C with a primary rabbit IgG anti-KCNJ15 antibody (Abcam, ab200397; 1:250), followed by washing and a 45-minute incubation with a secondary anti-rabbit-HRP antibody (1:3000; Merck Milipore). After final washing, the membrane was developed in the presence of an HRP substrate using a MicroChemi apparatus (DNR Bio-Imaging System). In the next step, antibodies bound to the membrane were removed using a 0.2 M NaOH solution, and a similar procedure was repeated with a primary mouse anti-GAPDH antibody (1:1000; Sigma–Aldrich) and a secondary anti-mouse-HRP antibody (1:3000; Bio–Rad). The development process was carried out as previously described [30].

2.10. Immunocytofluorescence staining and imaging

2.10.1. Kir4.2 immunodetection

3T3 fibroblasts were seeded onto cover glasses at a density of $4 \times 10^3/cm^2$ and cultured for 24 h. They were then fixed with 3.7 % formaldehyde in PBS for 20 min at room temperature (RT). After fixation, the cells were permeabilized with 0.01 % Triton X-100 for 5 min, and nonspecific binding sites were blocked with 3 % BSA in PBS for 60 min. Next, the cells were incubated overnight at 4 °C with a rabbit IgG anti-KCNJ15 antibody (Abcam, ab200397; 1:100). After washing, the cells were incubated with a secondary goat anti-rabbit antibody labelled with Alexa Fluor 568 (Abcam, ab175471; 1:100) and Hoechst 33258 (1 μg/ml; Life Technologies), all in PBS with 3 % BSA, for 60 min at RT. The cover glasses were thoroughly washed with water and then used to prepare specimens with fluorescence mounting medium (Dako).

Imaging of the prepared specimens was conducted using a Leica DMI6000B fluorescence microscope equipped with a PL APO 40×/1.25 OIL objective, a Leica DFC360FX CCD camera, and suitable filter cubes - the N2.1 (BP 535/44; 580; LP 590) and A4 (BP 360/40; 400; BP 470/40), controlled with LAS X 1.9 software.

2.10.2. EGFR distribution

3T3 fibroblasts were seeded onto sterile cover glasses measuring 60 × 10 × 0.2 mm (7×10^3 cells per glass in 250 μl of complete culture medium). After 24 h of culture, the glass was placed into an electrotactic observation chamber during assembly (constructed as previously described with minor modifications, as 60 × 10 × 0.2 mm glasses were doubled to accommodate an additional glass with cells). The electrotactic chamber was then assembled as described previously, and dcEF was applied to the cells for a specified time period.

Subsequently, the cover glass with cells was transferred to an ice-cold methanol:acetone (7:3) fixative solution (POCH) for 10 min, followed by washing. Nonspecific binding sites were blocked with 1 % BSA in PBS for 60 min. The cells were then incubated with rabbit anti-EGFR antibodies (1:250; Abcam, ab52894) overnight at 4 °C. After washing, the cells were incubated with goat anti-rabbit Alexa Fluor 488-conjugated antibodies (1:300; Life Technologies, A11008) and Hoechst 33258 (1 μg/ml; Life Technologies), all in PBS containing 1 % BSA, for 60 min. The cover glasses were thoroughly washed with water, and aqueous specimens were prepared for total internal reflection fluorescence (TIRF) microscopy.

The imaging was performed using a Leica DMI6000B microscope equipped with a TIRF module, a 488 nm diode laser, an HC PL APO 100×/1.47 OIL objective, and a Leica DFC360FX CCD camera. The system was controlled using LasX 3.4 software (All Leica, Wetzlar, Germany). Green fluorescence of stained EGFR was excited using a GFP-T ET filter cube (BP 470/40; 495; BP 525/50), and the penetration depth of the evanescent wave was set at 110 nm. Fluorescence signal profiles were generated using Fiji ImageJ 1.51n software [28].

2.11. Calcium level monitoring

Cells were seeded in the electrotactic chamber as previously described and loaded with Fluo-4-AM (ThermoFisher Scientific), with slight modifications to the protocol (2 μM for 60 min followed by washing). Fluorescence signals were recorded using the Leica DMI6000B microscope mentioned above, although standard epifluorescence was employed with a 5-s time interval. A dcEF of 3 V/cm was applied after the initial 2 min under isotropic conditions, reversed after 15 min and turned off after an additional 10 min. Five minutes later, ionomycin (10 μM; Life Technologies) was introduced into the culture medium as a positive control. The obtained image series were analysed using Fiji ImageJ 1.51n software [28], which utilized a custom-made macro to automatically measure the mean fluorescence intensity of cells over time, corresponding to intracellular calcium levels.

2.12. Screening for ion channel genes

To assess the involvement of specific ion channels in cellular electrotaxis, we used 227 sets of siRNA constructs from the Mouse ON-TARGETplus siRNA library - Ion Channels, SMARTpool (Dharmacon; Cat No. G-113805-01). siRNA solutions were prepared following the manufacturer's protocol, resulting in a 5 μM stock solution in 20 μl of 1× siRNA buffer (Dharmacon), which was stored frozen until use.

3T3 fibroblasts were seeded in 24-well plates (3×10^4 cells per well) in DMEM HG culture medium with 10 % FBS, excluding antibiotics. After 24 h, cells were transfected with Dharmafect I (Dharmacon) according to the provided protocol, using 1 μl of reagent and 2.5 μl of the specific siRNA stock solution per well. Twenty-four hours post-transfection, cells were reseeded on the basal glass of the electrotactic chamber (60 × 35 × 0.2 mm) using a 9-well PDMS stencil (alveole) placed in the middle at a cell density of 400 cells/9 mm^2 area in 10 μl of complete culture medium. Cells were kept in a humidity chamber until the experiment, which was conducted 48 h after transfection. At this point, the stencil was removed, and the electrotactic chamber was assembled as previously described.

In contrast to the basic approach, this setup allowed for the simultaneous time-lapse recording of eight different cell types with specific genes silenced, alongside control cells transfected with nontargeting siRNA. This was achieved using a fully motorized Leica DMi8 microscope equipped with an environmental chamber, an MC170-HD CMOS camera, and an HC FL PLAN 10×/0.25 DRY objective and operated with LAS X 3.7 software (all Leica, Wetzlar, Germany). Images from three

different fields of view for each condition were captured sequentially every 5 min for a duration of 4 h and 30 min. After the initial 30 min of recording, a dcEF of 3 V/cm was applied. Migration analysis was performed for 30 randomly selected cells for each condition. Directional cosine γ and speed of cell migration (normalized to the corresponding control cells) were plotted, and the conditions with the highest deviations from the mean for both parameters (i.e., the lowest and highest 2.5 % of cases) were designated as significant, as previously described [26].

2.13. Statistical analysis

The statistical analysis of the obtained results was conducted using Statistica 13.1 software (TIBCO Software). The statistical significance of the speed of cell migration, displacement, and CME was assessed using Student's *t*-test. The statistical significance of the parameter determining the directionality of movement (cos γ) was analysed using the nonparametric Mann–Whitney *U* test due to the distribution characteristics of the obtained results. Data are presented as the mean ± SEM. In each case, a p value < 0.05 was considered statistically significant.

3. Results

3.1. Electrotaxis of mouse 3T3 cells

In our first experiments, we confirmed that 3T3 fibroblasts show robust electrotactic activity. In the absence of an electric field, 3T3 cells showed random movement (cos γ = 0.054 ± 0.088) (Fig. 1, Supplementary Movie A). However, after the application of an electric field, the movement of the cells became strongly directional, and the cells turned

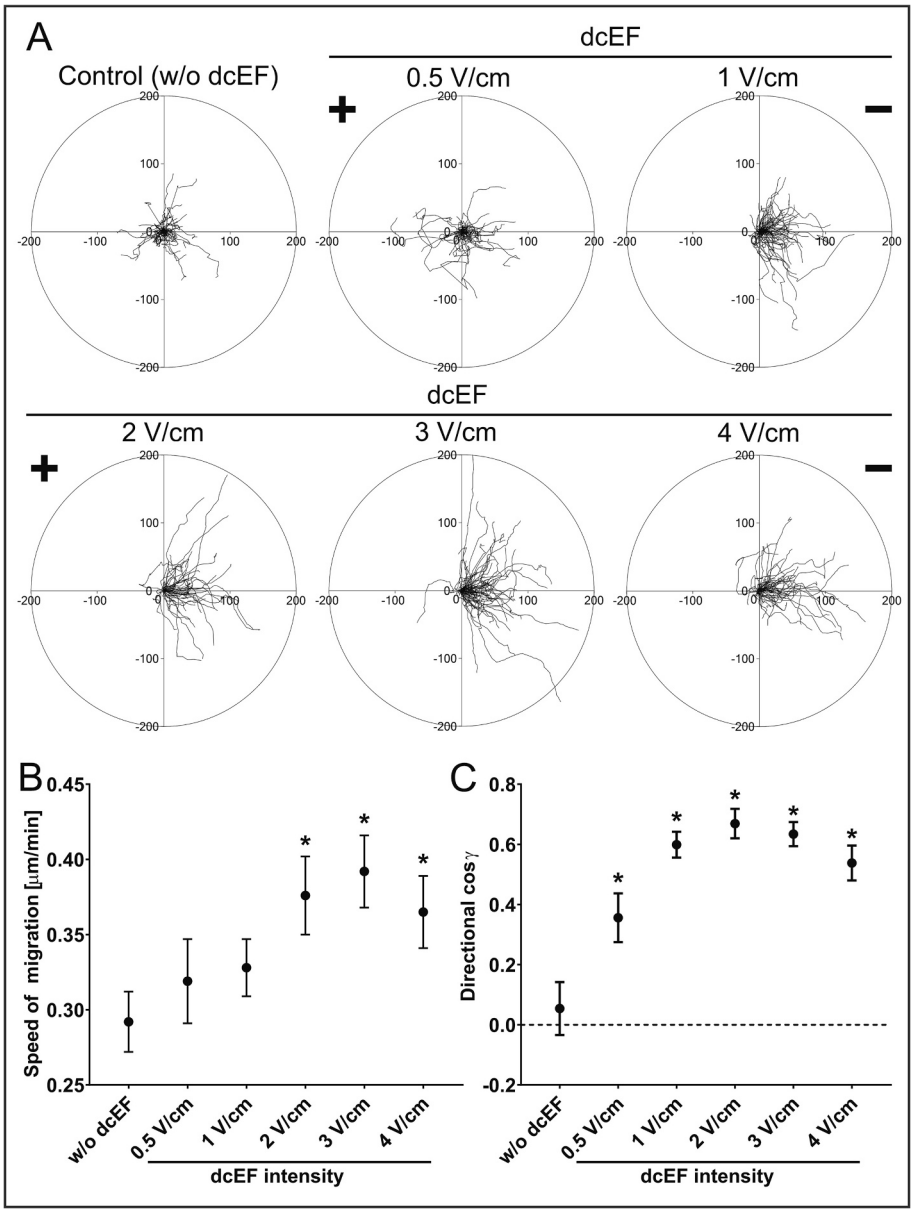

Fig. 1. Migration of 3T3 fibroblasts under isotropic conditions and in a direct-current electric field (dcEF) of physiological magnitude. (A) Circular diagrams showing composite trajectories of individual cell migration without dcEF and with a dcEF of 0.5–4 V/cm. The initial point of each trajectory (constructed from the subsequent 48 cell centroid positions, designated with a 5-minute interval) was moved to the beginning of the coordinate system. The cathode of dcEF (if present) is located on the right side of the diagram. The scale is in μm. (B) Speed of cell migration and (C) directionality of cell migration (presented as mean directional cos γ), calculated as the mean (for the analysed population) ± SEM. Cell numbers (*n*) are specified in Table 1. *Statistically significant differences relative to control (w/o dcEF) ($p < 0.05$).

towards the cathode (Fig. 1A). The effects of the electric field on the motility of 3T3 cells were enhanced as the applied voltage gradient was strengthened (Fig. 1A, B). As the electric field increased from 0.5 V/cm to 3 V/cm, the directionality of movement, the speed of movement and the average cell displacement increased steadily (Fig. 1B, C, Table 1, Supplementary Movies B, C). We also observed that the application of dcEFs resulted in a significant increase in cell movement efficiency (CME) compared to the control (Table 1).

3.2. The dynamics of the reaction of 3T3 cells to the electric field – analysis of cell trajectories

To determine the dynamics of the reaction of 3T3 cells to the electric field, we analysed the changes in the values of average directional cosines γ every 5 min after exposition of the 3T3 cells to an electric field of 3 V/cm. As shown in Fig. 2, 3T3 cells achieved maximum directionality of movement (directional cosine approximately 0.6) after approximately 60 min; however, the first clear changes in the value of the directional cosine were visible as early as 5 min after the electric field was turned on. As shown in Fig. 2 and Supplementary Movie D, the directionality of cell movement was completely reversible upon reversing the field polarity (3 V/cm). A complete reversal of the cell direction (that is, value of directional cosines γ approximately −0.6) after a change in dcEF polarity was observed after approximately 40 min. However, the first observed reaction (i.e., decrease in the value of directional cosine) after reversing the field polarity was much faster and was approximately 5 min. The obtained results could therefore suggest that the response of 3T3 fibroblasts to an electric field runs in the time interval of several minutes and, although it is relatively fast, it can still be explained by the relocation of membrane proteins.

3.3. The dynamics of the reaction of 3T3 cells to the electric field – analysis of cell morphology

More precise in the analysis of the dynamics of the cell reaction to the electric field than the determinations of the cell centroid position and calculation of the directional cosine seems to be the analysis of changes in cell morphology, i.e., the place and dynamics of lamellipodium formation and cell retraction [6]. For this reason, in subsequent experiments, we used a method based on measurements of changes in the surface of areas directed to individual poles of the electric field. Figs. 3 and 4 show the changes that the cell edges undergo in response to an applied electric field. Under control conditions (Fig. 3A), the process of migratory protrusion formation was not directed within the population of cells. Exposing the cells to the electric field causes the protrusion regions (green) to be located in a short time on the cathode side, whereas the retractable areas can be observed on the side facing the anode (red). Repolarization of individual cells after reversing the field polarity (Fig. 3B) varies in intensity due to their diversified morphology and migratory activity; however, they have a common feature for all, the first morphological changes occur within 2 min from changing the direction of the electric field.

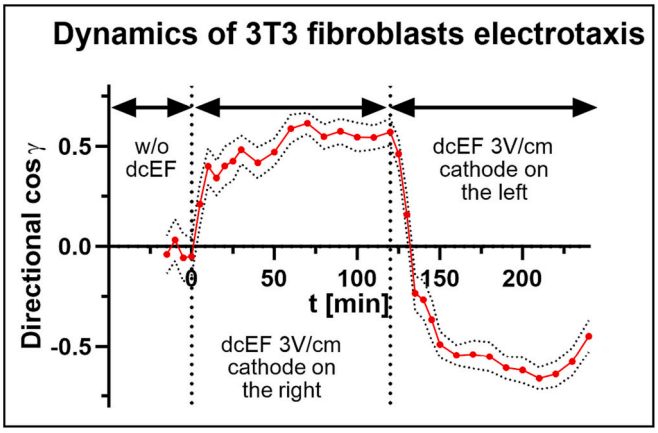

Fig. 2. The dynamics of the response of 3T3 fibroblasts to the application and reversal of dcEF. Directional cos γ was calculated at 5-min intervals for the analysed cell population ($n = 50$) and presented as the mean ± SEM. A 3 V/cm dcEF was applied at 0 min with the cathode on the right. After a subsequent 120 min, the dcEF was reversed (with electrode replacement), and the cathode was placed on the left side of the field of view.

Quantitative analysis of the primary response of 3T3 cells to an electric field is shown in Fig. 4B. An analogous analysis was performed for 3T3 cells after changing the direction of the electric field (Fig. 4C). Quantitative analysis of 3T3 cell responses to a change in electric field direction (Fig. 4C) revealed that on the left side of the cell that was originally directed to the anode (after replacing the electrodes to the cathode), the increase in area begins within 30–60 s after electrode replacement, while the retraction process performed on the opposite side of the cell starts with only a slight delay. Observation of the reaction manifested by a change in the dynamics of the leading edge and retraction of the back of the cell for approximately 1 min seems to be difficult to reconcile with hypotheses that try to explain cell electrotaxis only as a result of membrane protein lateral electrophoresis or electroosmosis.

3.4. The role of calcium signalling in the regulation of electrotaxis of 3T3 cells

The fast response of slowly migrating 3T3 cells to the change in the direction of the electric field suggests that the primary response of the cells to the electric field may be related to the activation of membrane ion channels rather than the translocation of cell membrane proteins. As calcium signalling has often been proposed to play an important role in the regulation of electrotaxis [31–35] in subsequent experiments, we tested the role of calcium ions in the electrotactic reaction of 3T3 fibroblasts.

To do this, the electrotactic reaction of 3T3 cells was tested in a calcium-free medium and in the presence of intra- and extracellular Ca^{2+} ion chelators (BAPTA-AM and EGTA, respectively). Voltage-gated calcium channels (VGCCs) were also inhibited using the inhibitor verapamil (at a concentration of 50 μM). Finally, the activity of MLCK kinase, which is the main signalling element that links calcium ion influx into the cytoplasm with the migration of cells, was inhibited using the ML7 inhibitor (at a concentration of 10 μM) (Fig. 5, Table 2).

The results of the experiments did not confirm the participation of calcium ions in the electrotactic reaction of 3T3 cells (Fig. 5, Table 2). In no case was the decrease in directionality of migration statistically significant. The use of chelators resulted in a reduction in the speed of movement, which may, to some extent, hinder the interpretation of the results; however, as shown in the enlarged fragment of the chart, the decrease in migration activity did not result in disturbance of the directional movement.

Since the most frequently postulated mechanism for the role of calcium ions in the electrotactic reaction is the induction of the influx of these ions from outside of the cells under the influence of an electric field, in subsequent experiments, we observed changes in the level of Ca^{2+} ions in cells exposed to the electric field (Fig. 5D). It has been shown that the electric field of physiological intensity does not cause the influx of calcium ions to the tested cells or an increase in the calcium concentration at the expense of intracellular stores. Both the field application and the subsequent change in its direction did not cause changes in the calcium level (Fig. 5D).

3.5. The role of inwardly rectifying K^+ channel Kir4.2 in the regulation of 3T3 cell electrotaxis

The ion mechanisms that may be responsible for the rapid response

Table 1
Migration of 3T3 fibroblasts in isotropic conditions and in a direct-current electric field (dcEF).

	dcEF intensity [V/cm]					
	w/o ($n = 43$)	0.5 ($n = 50$)	1 ($n = 71$)	2 ($n = 50$)	3 ($n = 70$)	4 ($n = 55$)
Speed of migration [μm/min]	0.292 ± 0.020	0.319 ± 0.028	0.328 ± 0.019	0.376 ± 0.026*	0.392 ± 0.024*	0.365 ± 0.024*
Displacement [μm]	32.477 ± 3.963	36.830 ± 3.949	50.520 ± 3.832*	67.616 ± 5.756*	68.062 ± 5.395*	60.977 ± 5.282*
CME	0.442 ± 0.039	0.503 ± 0.037	0.630 ± 0.030*	0.739 ± 0.024*	0.696 ± 0.022*	0.667 ± 0.027*
Cosine γ	0.054 ± 0.088	0.356 ± 0.081*	0.599 ± 0.043*	0.669 ± 0.049*	0.634 ± 0.040*	0.538 ± 0.058*

* Statistically significant differences relative to control (w/o dcEF) ($p < 0.05$).

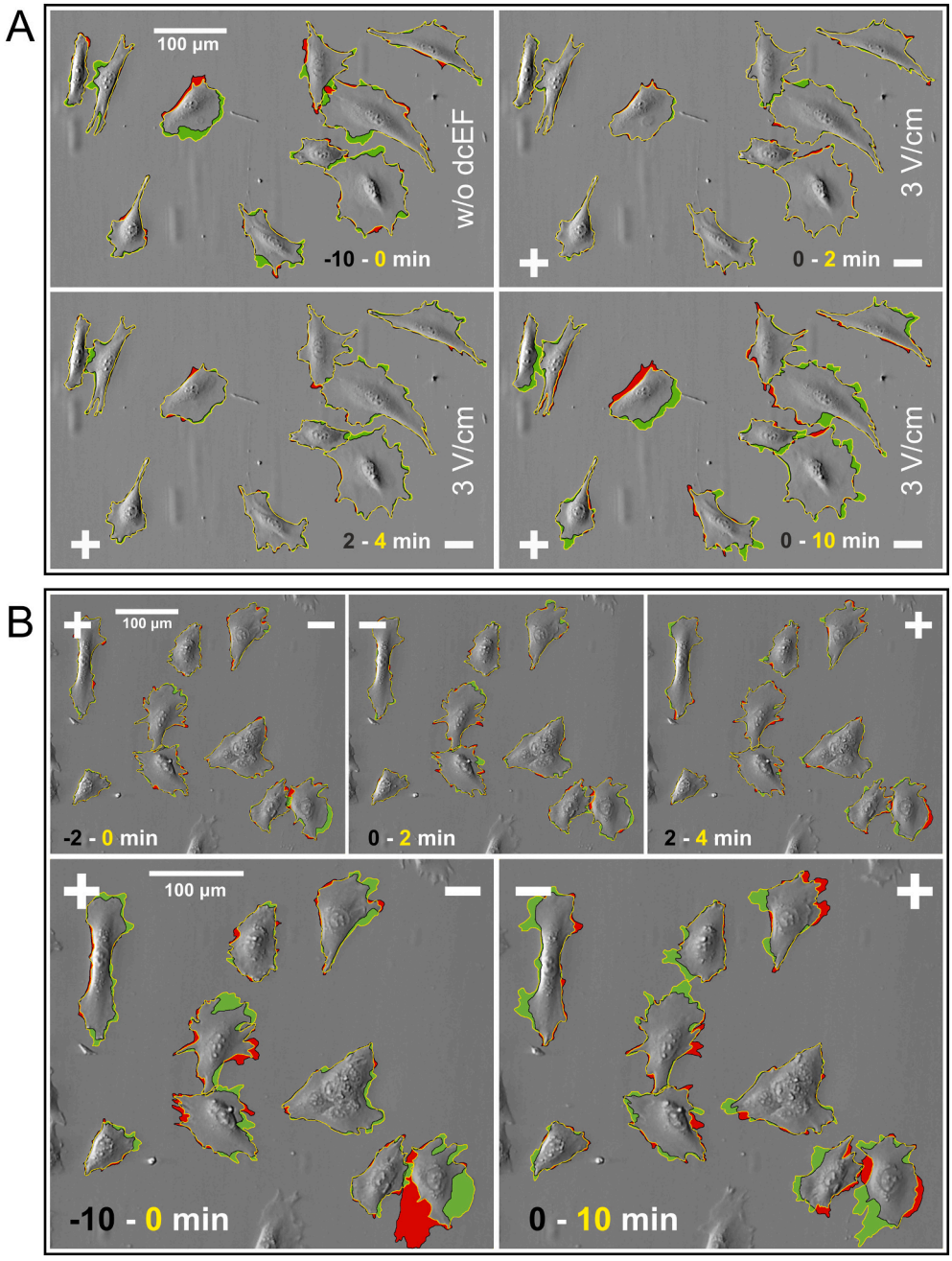

Fig. 3. The dynamics of the response of 3T3 fibroblasts to dcEF application (A) and reversal (B) analysed based on cell morphology. Image sequences show changes in cell morphology between subsequent time points. The regions of protrusion formed within a given time interval are marked in green, while the regions released during cell retraction are marked in red. In Panel (A), a dcEF is applied (at time point 0 min) with the cathode on the right, while in Panel (B), the dcEF is reversed (at time point 0 min) and the cathode is located on the left.

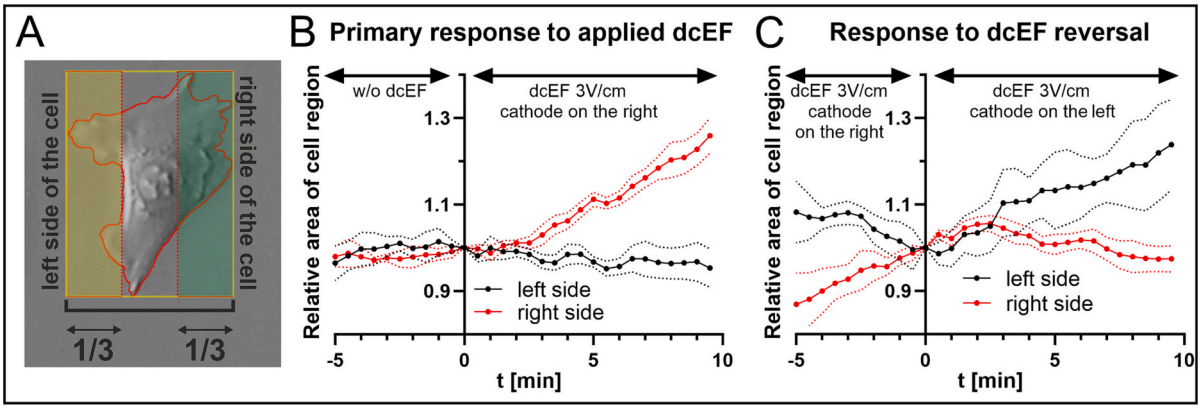

Fig. 4. Quantitative analysis of 3T3 fibroblast electrotaxis according to morphology. The analysis was carried out as presented in Panel (A), where the cell is divided into three equal regions along the axis parallel to the electric field lines. The areas of the specified regions, namely, the 'left side' and 'right side of the cell', were measured and plotted. The cell response to the application and reversal of dcEF is shown in Panels (B) and (C), respectively. During the primary response to the applied dcEF, the right side of the cell faces the cathode. After the reversal of the dcEF, the left side faces the cathode. The relative cell area is normalized to the area measured at time 0 s (the time of dcEF application (B) or reversal (C)). The area of the cell region was calculated at 30 s time intervals and is presented as the mean ± SEM ($n = 12$).

of cells to dcEF are not limited to the aforementioned calcium ions. RNAi screening revealed that in epithelial cells, the inwardly rectifying K^+ channel Kir4.2 plays a particularly important role in sensing the electric field [26]. The importance of this channel for the persistence of migration of fibroblasts was also suggested by de Hart et al. [36].Therefore, we tested the potential role of these channels in the regulation of electrotaxis of 3T3 fibroblasts. In the first experiment, we used Ba^{2+}, a broad-range blocker for a family of Kir channels [37]. As shown in Fig. 6 and Table 3, Ba^{2+} inhibited electrotaxis of 3T3 cells in a dose-dependent manner; however, a statistically significant decrease in directional cosine was observed in the presence of 500 μM $BaCl_2$ (Fig. 6C). Importantly, $BaCl_2$ at this concentration only slightly reduced the speed of migration of 3T3 cells (Fig. 6B). Interestingly, the inhibitory effect of blocking the Kir channel on cell electrotaxis was much stronger in the first hour of the experiment than in the entire 4-hour experiment (Fig. 6D).

Since this observation might suggest that these channels may be responsible only for the first rapid response of cells to the electric field, we analysed the kinetics of the response of $BaCl_2$-treated 3T3 cells to dcEF throughout the entire experiment (Fig. 6E, F).

The analysis of kinetics revealed that in a field with an intensity of 1 V/cm, 500 μM $BaCl_2$ (Fig. 6E) not only disturbs the rate of the primary reaction of cells to the electric field but also inhibits the directionality of motion throughout the experiment. On the other hand, in the case of an electric field of 3 V/cm (Fig. 6F) for the first 30 min, the movement of cells is completely random, after which the cells gradually regain the ability to migrate towards the cathode; however, directionality close to the control conditions (3 V/cm) is achieved only after 150 min. This result may suggest that in stronger dcEF, another mechanism may compensate for the inhibition of Kir channels after a prolonged period of time.

Inwardly rectifying potassium channels (Kir) mediate the inwards flow of K^+ ions at hyperpolarizing membrane voltages more readily than the outwards flow of K^+ at depolarizing voltages as the result of the blockage of the channel by intracellular polyamines such as spermine (SPM) and spermidine (SPD) or magnesium ions, which interact with negatively charged amino acid residues of Kir channels exposed inside the cell and prevent the flow of potassium ions from the cell. In subsequent experiments, the effect of modification of the level of these intracellular Kir channel regulators on the electrotactic activity of 3T3 cells was investigated. Preincubation of cells with an analogue of intracellular polyamines, DENSPM, results in the induction of SPM/SPD acetyltransferase (SSAT) and a subsequent reduction in intracellular polyamines. The opposite effect is caused by preincubation of cells with putrescine, a polyamine that only slightly regulates Kir activity but is processed within cells into spermine and spermidine, polyamines with much greater activity [36,38].

As shown in Fig. 7 and Table 4, lowering the level of intracellular polyamines significantly reduced the directionality of cell migration in both the 1 V/cm and 3 V/cm fields (Fig. 7D). In contrast, increasing the level of intracellular polyamines by preincubation with putrescine resulted in a slight increase in directionality with each tested field strength (indicating a small effect size based on Cohen's d, a statistical measure of effect magnitude). Importantly, the substances tested did not inhibit the speed of migration (Fig. 7C).

In addition to polyamines, intracellular magnesium ions can also be a factor regulating the activity of Kir channels. To verify their participation in the regulation of electrotaxis of 3T3 fibroblasts, magnesium chloride was added to the cells treated with dcEF. Interestingly, the application of Mg^{2+} ions at a concentration of 10 mM led to a clear decrease in the directionality of cell movement without affecting migration speed (Fig. 8, Table 5). It should be emphasized that incubation of cells with 10 mM $MgCl_2$ causes a significant increase in the concentration of Mg^{+2} ions within the cell (Fig. 8D). As Nakajima et al. [26] suggested that during electrotaxis extracellular dcEFs redistribute positively charged polyamines, which then asymmetrically bind to Kir4.2 to regulate the K^+ fluxes, it can be speculated that the high concentration of magnesium ions in the cytoplasm may mask the effect of asymmetrically redistributed polyamines induced by dcEF and inhibit directional movement.

The results obtained indicated that inwardly rectifying K^+ Kir channels are involved in the regulation of 3T3 cell electrotaxis. However, Nakajima et al. [26] showed that within this channel family, the KCNJ15/Kir4.2 channel is particularly important for epithelial cell electrotaxis. Therefore, in subsequent experiments, we investigated the specificity of inwardly rectifying Kcnj15/Kir4.2 channels in dcEF sensing by 3T3 fibroblasts. As shown in Fig. 9 Table 6 and Supplementary Movie E, 3T3 cells after Kcnj15 knockdown lost directional migration in the electric field but maintained the same migration speed as nontarget siRNA control cells or cells without dcEF. Inhibition of the expression of the Kcnj15 gene, which encodes the Kir4.2 channel, had a clear impact on the directionality of migration of 3T3 cells in a field of 1 V/cm. The decrease in directional cosine γ to the level of 0.218 is statistically significant and, importantly, is not accompanied by impairment in cell migration activity. A smaller but also a statistically significant effect of inhibition of directional movement was observed in

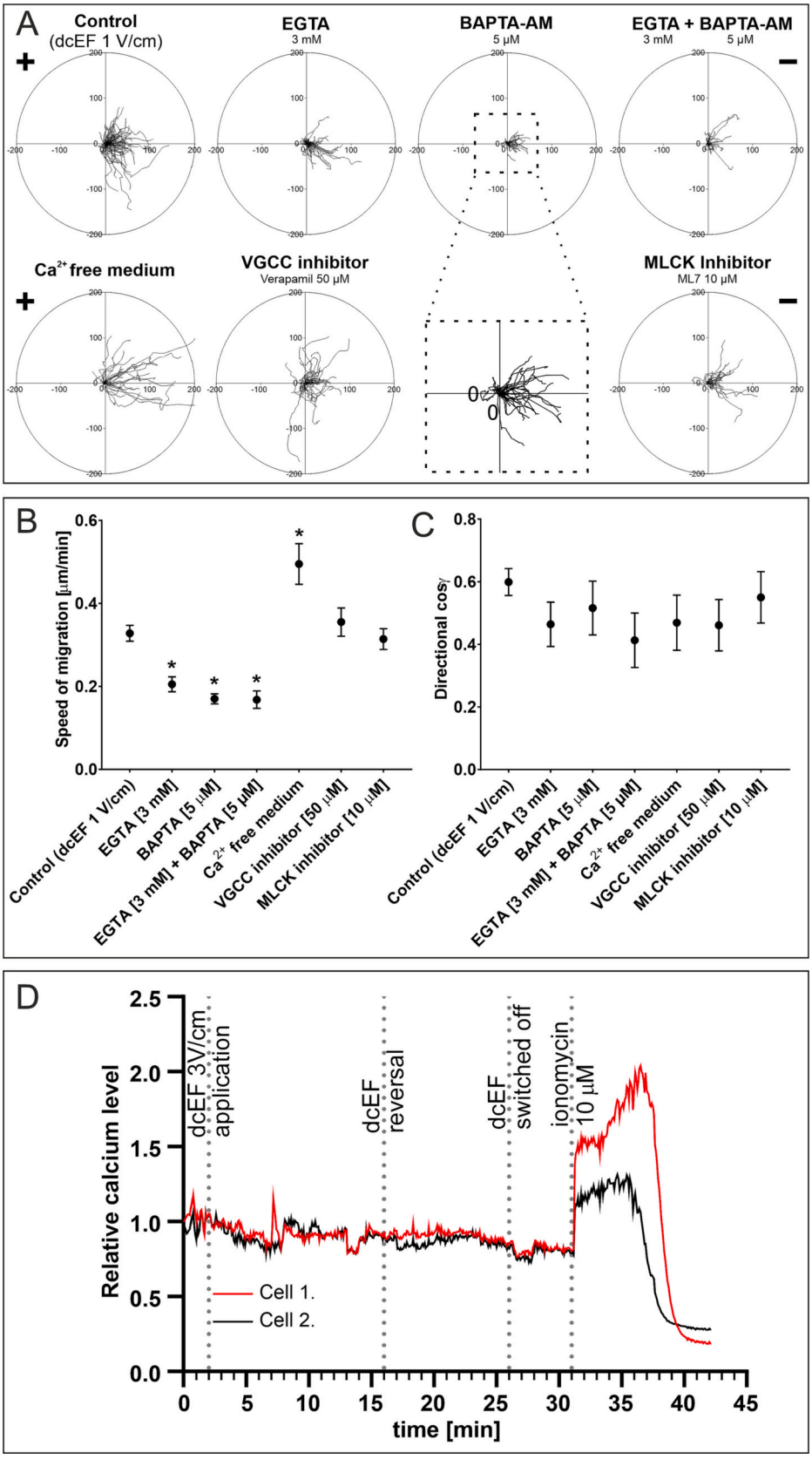

(caption on next page)

Fig. 5. The role of calcium signalling in the electrotaxis of 3T3 fibroblasts. (A) Circular diagrams presenting composite cell trajectories under different conditions: control conditions (dcEF 1 V/cm), in culture medium without calcium ions, in the presence of intracellular and extracellular Ca^{2+} ion chelators (BAPTA-AM 5 μM and EGTA 3 mM, respectively), VGCC and MLCK inhibitors (Verapamil 50 μM and ML7 10 μM, respectively). Diagrams were constructed as previously described (see Fig. 1). Additionally, the central region of the diagram for electrotaxis in the presence of BAPTA-AM was enlarged to visualize directional, although slow, migration. (B) Speed of cell migration and (C) Directionality of cell migration (presented as directional cos γ), calculated as the mean (for the analysed population) ± SEM. Cell numbers (*n*) are specified in Table 2. *Statistically significant differences relative to the control (dcEF 1 V/cm) ($p < 0.05$) (D) Monitoring of intracellular calcium levels during electrotaxis of 3T3 fibroblasts. Cells were loaded with Fluo4-AM and visualized via fluorescence microscopy during dcEF of 3 V/cm application, reversal and turning off. An ionophore (ionomycin 10 μM) was subsequently applied as a positive control. Two independent cells were analysed, and for each, the fluorescence level was normalized to a value of 1 at the initial point of registration.

Table 2
The role of calcium signalling in the electrotaxis of 3T3 fibroblasts.

	Control (dcEF 1 V/cm) (*n* = 71)	EGTA (3 mM) (*n* = 49)	BAPTA-AM (5 μM) (*n* = 29)	EGTA (3 mM) + BAPTA-AM (5 μM) (*n* = 26)	Ca^{2+} free medium (*n* = 30)	VGCC Inhibitor – Verapamil (50 μM) (*n* = 37)	MLCK Inhibitor – ML7 - (10 μM) (*n* = 25)
Speed of migration [μm/min]	0.328 ± 0.019	0.205 ± 0.018*	0.170 ± 0.012*	0.168 ± 0.021*	0.495 ± 0.049*	0.355 ± 0.034	0.314 ± 0.025
Displacement [μm]	50.520 ± 3.832	34.067 ± 4.055*	26.427 ± 2.705*	26.783 ± 4.717*	90.938 ± 10.674*	50.142 ± 5.874	51.389 ± 6.234
CME	0.630 ± 0.030	0.649 ± 0.035	0.641 ± 0.046	0.600 ± 0.046	0.737 ± 0.029*	0.610 ± 0.037	0.663 ± 0.047
Cosine γ	0.599 ± 0.043	0.464 ± 0.071	0.516 ± 0.086	0.413 ± 0.087	0.469 ± 0.088	0.461 ± 0.082	0.550 ± 0.082

* Statistically significant differences relative to control (dcEF 1 V/cm) ($p < 0.05$).

the case of a dcEF with an intensity of 3 V/cm.

Analysis of the kinetics of the reaction of 3T3 cells to dcEF after Kcnj15 knockdown showed that it is identical to the pharmacological inhibition of Kir channels with $BaCl_2$ (Figs. 9F, G and 6E, F). The results obtained clearly indicate that the Kcnj15/Kir4.2 channel is responsible for dcEF sensing by 3T3 fibroblasts.

3.6. Other ion channels involved in the fast electrotactic reaction of 3T3 cells

Electrotaxis was shown in the past to depend not only on the activity of calcium channels or inwardly rectifying K^+ channel Kir4.2 but also on several other types of ion channels [7,19,26]. To verify the role of other ion channels in the electrotaxis of 3T3 cells, we used the large-scale screening method described by Nakajima et al. [26]. We employed the ON-TARGETplus siRNA mouse ion channel siRNA library and analysed 227 sets of siRNAs against genes that encode mouse ion channels. The effects of knockdown of specific genes on the speed of migration and directionality of movement are presented in Fig. 10. To identify which gene knockdowns showed significant effects on migration speed and directional cosine, we set cut-off lines at 2.5 % of the population distribution of both the directionality and speed values after knockdown [26]. We found 22 gene knockdowns that showed significant effects on electrotaxis of 3T3 cells. The 10 identified genes significantly affected the directionality of migration in dcEF without a significant effect on the speed of movement. Knockdown of Kcnj15, Kcnmb2 (potassium large conductance calcium-activated channel, subfamily M, beta member 2), Fxyd1 (FXYD domain-containing ion transport regulator 1), Pkd1l3 (polycystic kidney disease 1 like 3), Catsper1 (cation channel, sperm associated 1) and Chrnb1 (cholinergic receptor nicotinic beta 1 subunit) decreased directionality of movement, while knockdown of Clcn6 (chloride channel, voltage-sensitive 6), Gabrd (gamma-aminobutyric acid (GABA) A receptor, subunit delta), Trpc5 (transient receptor potential cation channel, subfamily C, member 5), Kcnh8 (potassium voltage-gated channel, subfamily H (eag-related), member 8) and Scn2a1 (sodium channel, voltage-gated, type II, alpha) increased directionality of movement. However, careful analysis of all data (Supplementary Table A) clearly indicates that many more types of ion channels are involved in electrotaxis regulation, including K^+, Na^+, Ca^{2+} and Cl^- channels. The presented data confirm the crucial role of Kcnj15 in electrotaxis of 3T3 cells and demonstrate that electric field sensing is the result of the interaction of many types of ion channels.

3.7. Biphasic mechanism of electrotaxis of mouse 3T3 fibroblasts: complementary role of ion channels and chemoattractant receptors?

One of the most intriguing observations presented in this paper was the statement that inhibition of the Kir4.2 channel abolishes the directional movement of 3T3 cells in dcEF, but only for the first 1–2 h of the experiment. Subsequently, we observed the reappearance of electrotaxis. It is possible that after a longer time, the lack of Kcnj15 channel activity may be compensated by other ion channels; however, the second possible explanation is that for the first fast cell reaction, the activity of Kir4.2 channels was critical, but after an appropriate period of time, receptor translocation in the cell membrane took over the leading role in the induction of directional movement. However, this hypothesis assumes that after approximately 40 min, electrostatic or electro-osmotic forces redistribute charged components of the cell membrane, including receptors for chemoattractants, and this increase in the density of membrane receptors on the cathode facing side of the cell would be responsible for the reappearance of electrotaxis in cells in which Kir4.2 channels were inhibited. To verify this hypothesis, we analysed the kinetics of the redistribution of 3T3 cell membrane proteins in dcEF of 1 V/cm and 3 V/cm. Since relocation of the EGF receptor was previously shown to be an important factor responsible for electrotaxis of various types of cells [17,39,40], in subsequent experiments, we examined whether there was a clear displacement of this receptor in dcEF in 3T3 cells at the time of our interest. The results presented in Fig. 11 show that after 30–60 min in a dcEF with an intensity of 3 V/cm, there is a clear accumulation of EGF receptors on the cell side of the cathode (Fig. 11C). Interestingly, such accumulation was much weaker in dcEF with an intensity of 1 V/cm (Fig. 11B). It is noteworthy that the transient effect of inhibition of the Kir4.2 channel on the directional movement of 3T3 cells was much more pronounced at 3 V/cm than at 1 V/cm (Figs. 6E, F and 9F, G). Since inhibition of the signalling pathway from the EGF receptor (AG1478 3 μM and LY294002 50 μM, EGFR and PI3K inhibitors, respectively) (Fig. 11D, F) was also found to partially inhibit 3T3 fibroblast electrotaxis, this hypothesis seems plausible but requires further research.

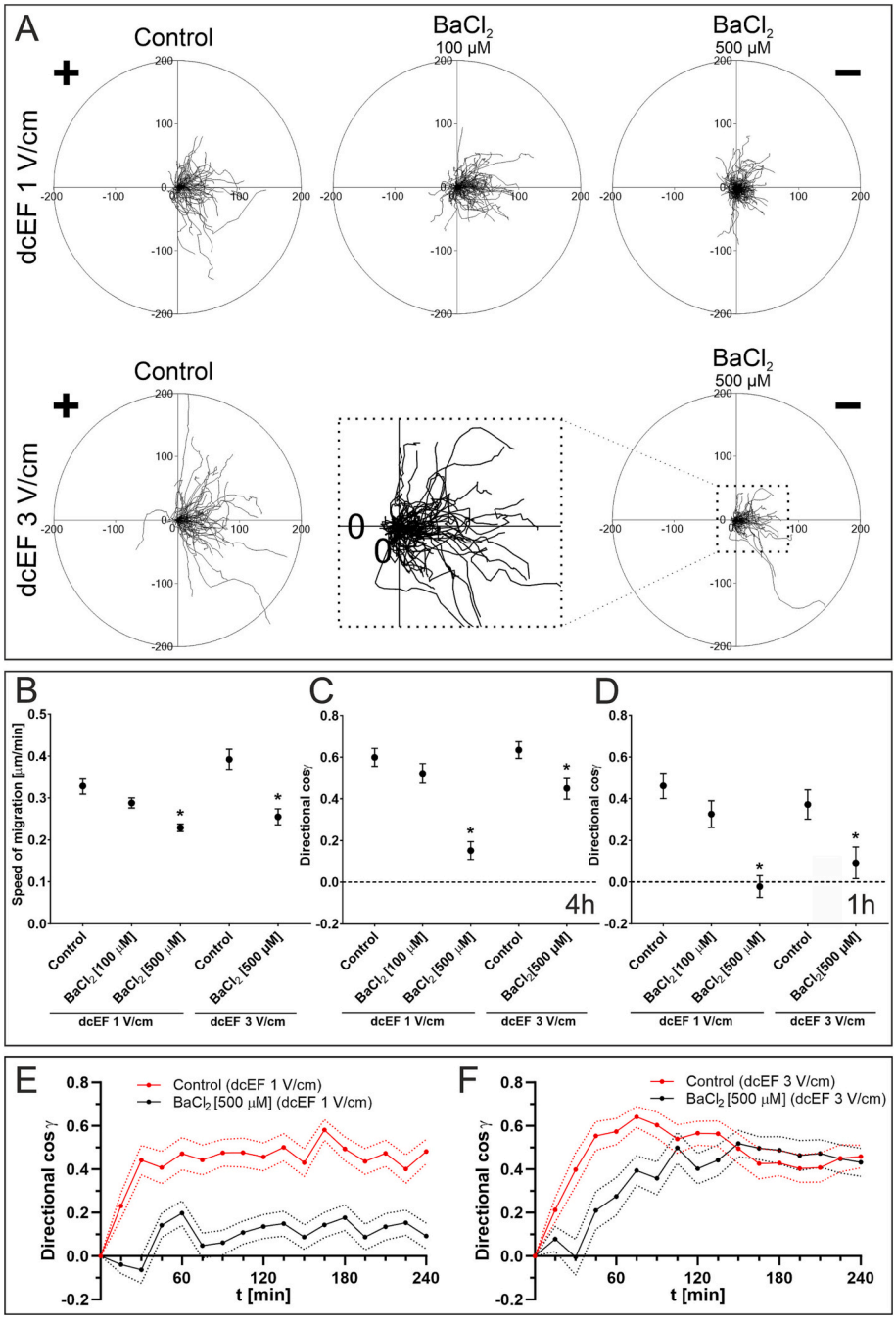

Fig. 6. The effect of pharmacological inhibition (with $BaCl_2$) of inwardly rectifying potassium channels on electrotaxis of 3T3 fibroblasts. (A) Circular diagrams presenting composite cell trajectories under different conditions: control conditions (dcEF 1 V/cm and 3 V/cm) and in culture medium with $BaCl_2$ at specified concentrations. Diagrams were constructed as previously described (see Fig. 1). Additionally, the central region of the diagram for electrotaxis in 3 V/cm and $BaCl_2$ (500 μM) was enlarged to visualize an initial delay of the directional response. (B) Speed of cell migration, and (C, D) Directionality of cell migration (presented as directional cos γ), calculated as the mean (for the analysed population) ± SEM. Panel (C) shows directionality of movement for the entire 4-hour experiment, while Panel (D) shows cos γ calculated only for the 1st hour since dcEF application. Cell numbers (*n*) are specified in Table 3. *Statistically significant differences relative to corresponding controls (either dcEF 1 V/cm or 3 V/cm) ($p < 0.05$). (E, F) Dynamics of electrotaxis in the presence of $BaCl_2$ (500 μM) in a dcEF of 1 V/cm and 3 V/cm, respectively, compared to control conditions, calculated as the mean directional cos γ ± SEM, with a 15-min time interval. Cell numbers (*n*) are specified in Table 3.

4. Discussion

Electrotaxis mechanisms have been extensively investigated but are still poorly understood, and no single "sensor" for electrotaxis has yet been identified. To date, the search for the primary electric field sensor in the cell has focused mainly on receptors for chemoattractants or other cell membrane proteins that would be moved to one side of the cell under the influence of the electric field or ion channels activated as a result of depolarization/hyperpolarization of the cell membrane on one side of a cell or as a result of mechanical effects induced by dcEF [15,41]. Because the relocation of the receptors in the cell membrane takes much longer than the activation of ion channels, an important factor in the search for a potential primary electric field sensor in the cell membrane is the dynamics of the cell's response to the electric field. According to various reports from the literature, the time required for the relocation of membrane proteins in dcEF at physiological intensity ranges from

Table 3
The effect of pharmacological inhibition (with $BaCl_2$) of inwardly rectifying potassium channels on electrotaxis of 3T3 fibroblasts.

	dcEF 1 V/cm			dcEF 3 V/cm	
	Control ($n = 71$)	$BaCl_2$ (100 μM) ($n = 98$)	$BaCl_2$ (500 μM) ($n = 125$)	Control ($n = 70$)	$BaCl_2$ (500 μM) ($n = 62$)
Speed of migration [μm/min]	0.328 ± 0.019	0.288 ± 0.012	0.229 ± 0.009*	0.392 ± 0.024	0.255 ± 0.019*
Displacement [μm]	50.520 ± 3.832	42.975 ± 2.670	24.931 ± 1.647*	68.062 ± 5.395	37.159 ± 3.888*
CME	0.630 ± 0.030	0.591 ± 0.023	0.444 ± 0.020*	0.696 ± 0.022	0.583 ± 0.027*
Cosine γ	0.599 ± 0.043	0.522 ± 0.047	0.152 ± 0.043*	0.634 ± 0.040	0.450 ± 0.052*

* Statistically significant differences relative to corresponding controls (either dcEF 1 V/cm or 3 V/cm) ($p < 0.05$).

several minutes to approximately 2 h [15,16,42–45]. In the same cases, a significant redistribution of membrane receptors was observed after approximately 10 min from the action of an electric field (for example, for EGF receptor) [17], and the same time was predicted by the mathematical flux model for a 30 μm diameter cell [18]. However, in our previous papers, we demonstrated that the initial reaction of some cells to electric fields is relatively fast [6,7]. For example, in *Amoeba proteus*, primary cell responses occurred <1 s after reversal of dcEF polarity [6]. The reaction was also relatively fast (approximately 30 s) in some tissue cells characterized by rapid migration [7,21,22]. As these observations suggested that in these rapidly migrating cells, activation of ion channels is a more likely dcEF sensor than receptor relocation, we decided to analyse the dynamics of the response to dcEF of slowly migrating cells such as 3T3 fibroblasts.

Our results clearly show that even in slowly migrating cells, the reaction for dcEF is relatively fast. Although the analysis of cell trajectories (directional cosine) suggests that the response of 3T3 fibroblasts to dcEF runs in the time interval of several minutes (Fig. 2) and therefore is consistent with the time needed for a clear accumulation of receptors on one side of the cell in dcEF [18], measurements of the dynamics of cell reactions for dcEF by analysis of extending and retracting cell regions clearly show that the primary reaction of the cell for electric field is more dynamic and begins within 30–60 s after reversal of the dcEF (Fig. 4B).

Because this time seems to be too short for a clear accumulation of the receptors on one side of the cell in dcEF, especially in the case of relocation of membrane receptors from one side of the cell (where they were previously displaced during movement in dcEF) to the opposite side after dcEF reversal, it seems more likely that the primary mechanism of electrotactic reaction is related rather to activation of ion channels than to cell membrane receptor translocation.

Ca^{2+} channels were among the first ion channels proposed to play an essential role in the electrotactic response [19]. Interestingly, the results of our experiments did not confirm the participation of calcium ions in the electrotactic reaction of 3T3 cells (Fig. 5, Table 2). Thus, our results confirmed the observation of Brown and Loew [46], that the electrotaxis of 3T3 cells does not depend on calcium ions. The calcium ion dependence of electrotaxis has been observed in several types of cells, including neural crest cells, *Dictyostelium discoideum*, and fish and human keratocytes [23,32–35,47]. However, the role of calcium ions in

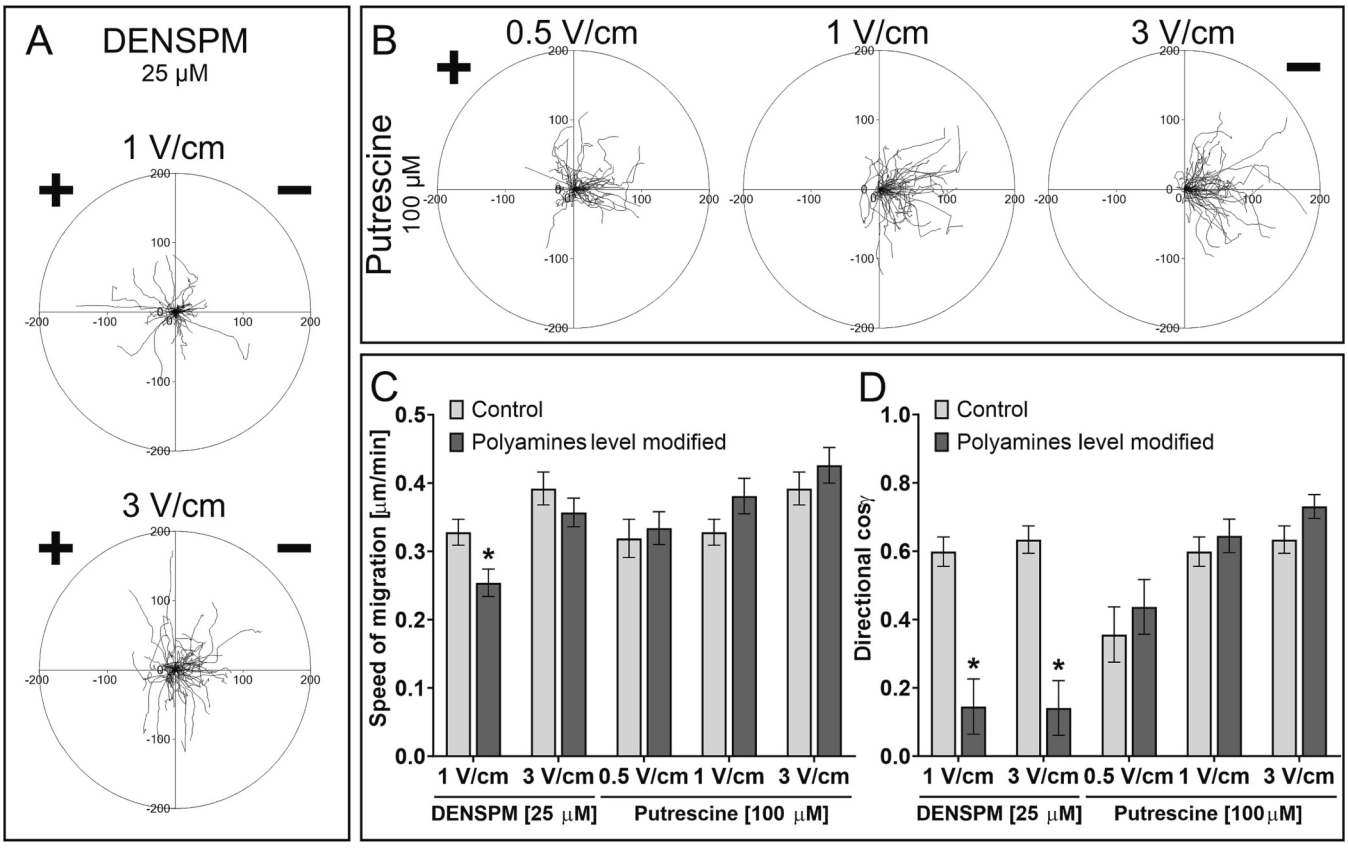

Fig. 7. The effect of modified levels of polyamines (SPM/SPD - main regulators of inwardly rectifying potassium channels) on electrotaxis of 3T3 fibroblasts. (A, B) Circular diagrams presenting composite cell trajectories after preincubation with (A) DENSPM (25 μM), leading to a decreased level of SPM/SPD, or with (B) putrescine (100 μM), causing the opposite effect. Diagrams were constructed as previously described (see Fig. 1). (C) Speed of cell migration, and (D) Directionality of cell migration (presented as directional cos γ), calculated as the mean (for the analysed population) ± SEM. Cell numbers (n) are specified in Table 4. *Statistically significant differences relative to corresponding controls (unmodified level of polyamines, dcEF 0.5, 1 or 3 V/cm) ($p < 0.05$).

Table 4
The effect of modified levels of polyamines (SPM/SPD - main regulators of inwardly rectifying potassium channels) on the electrotaxis of 3T3 fibroblasts.

dcEF intensity	Polyamines level unmodified			DENSPM (25 μM)		Putrescine (100 μM)		
	0.5 V/cm (n = 50)	1 V/cm (n = 71)	3 V/cm (n = 70)	1 V/cm (n = 51)	3 V/cm (n = 58)	0.5 V/cm (n = 50)	1 V/cm (n = 54)	3 V/cm (n = 50)
Speed of migration [μm/min]	0.319 ± 0.028	0.328 ± 0.019	0.392 ± 0.024*	0.254 ± 0.020*	0.357 ± 0.021	0.334 ± 0.024	0.381 ± 0.026	0.426 ± 0.026
Displacement [μm]	36.830 ± 3.949	50.520 ± 3.832*	68.062 ± 5.395*	40.266 ± 4.443	53.698 ± 4.635*	47.232 ± 4.469	61.604 ± 5.120	74.267 ± 5.443
CME	0.503 ± 0.037	0.630 ± 0.030*	0.696 ± 0.022*	0.615 ± 0.029	0.607 ± 0.030*	0.581 ± 0.033	0.674 ± 0.030	0.721 ± 0.023
Cosine γ	0.356 ± 0.081*	0.599 ± 0.043*	0.634 ± 0.040*	0.145 ± 0.081*	0.141 ± 0.080*	0.437 ± 0.080	0.645 ± 0.049	0.731 ± 0.035

* Statistically significant differences relative to corresponding controls.

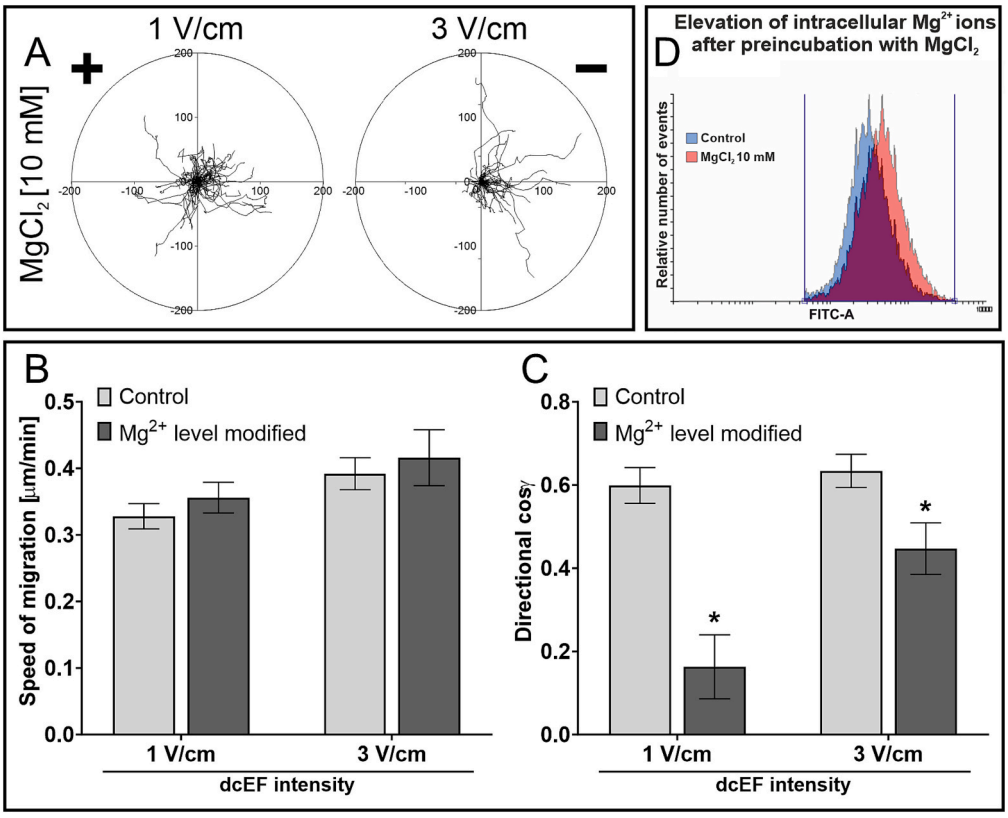

Fig. 8. The effect of modified intracellular Mg^{2+} ion levels (which regulate the activity of inwardly rectifying potassium channels) on the electrotaxis of 3T3 fibroblasts. (A) Circular diagrams presenting composite cell trajectories after preincubation with $MgCl_2$ (10 mM). Diagrams were constructed as previously described (see Fig. 1). (B) Speed of cell migration and (C) directionality of cell migration (presented as directional cos γ), calculated as the mean (for the analysed population) ± SEM. Cell numbers (n) are specified in Table 5. *Statistically significant differences relative to corresponding controls (unmodified levels of intracellular Mg^{2}, either in dcEF 1 or 3 V/cm) ($p < 0.05$). (D) Cytometric analysis of cells loaded with Mag-Fluo-4AM preincubated with $MgCl_2$ (10 mM) compared to control cells.

Table 5
The effect of modified intracellular Mg^{2+} ion levels on the electrotaxis of 3T3 fibroblasts.

	Unmodified Mg^{2+} level		$MgCl_2$ (10 mM)	
dcEF intensity	1 V/cm (n = 71)	3 V/cm (n = 70)	1 V/cm (n = 67)	3 V/cm (n = 44)
Speed of migration [μm/min]	0.328 ± 0.019	0.392 ± 0.024	0.356 ± 0.023	0.416 ± 0.042
Displacement [μm]	50.520 ± 3.832	68.062 ± 5.395	41.743 ± 3.643	61.951 ± 8.401
CME	0.630 ± 0.030	0.696 ± 0.022	0.495 ± 0.026*	0.565 ± 0.031*
Cosine γ	0.599 ± 0.043	0.634 ± 0.040	0.163 ± 0.077*	0.447 ± 0.062*

* Statistically significant differences relative to corresponding controls.

the electrotaxis of fibroblasts is not clear. For example, electrotaxis of mouse C3H/10 T1/2 fibroblasts is inhibited by calcium channel inhibitors or by the removal of extracellular calcium [33]. Moreover, Gou et al. [25] demonstrated that calcium ion flow promoted the migration of newborn mouse skin fibroblasts towards the cathode. However, Brown and Loew [46] demonstrated that 3T3 fibroblasts exhibit electrotaxis independent of Ca^{2+} signalling, and Ross et al. [48] showed that the Ca^{2+} channel blockers lanthanum and verapamil did not have a significant effect on the alignment of human gingival fibroblasts in the electric field. Therefore, it seems that the role of specific ions in electrotaxis is strongly dependent on the type and origin of cells. Interestingly, a large-scale screening method that we used to identify ion channel genes that are important in the electrotaxis of 3T3 cells revealed that siRNA against some calcium channels significantly inhibits the electrotaxis of 3T3 cells (Fig. 10, Supplementary Data Table A). This

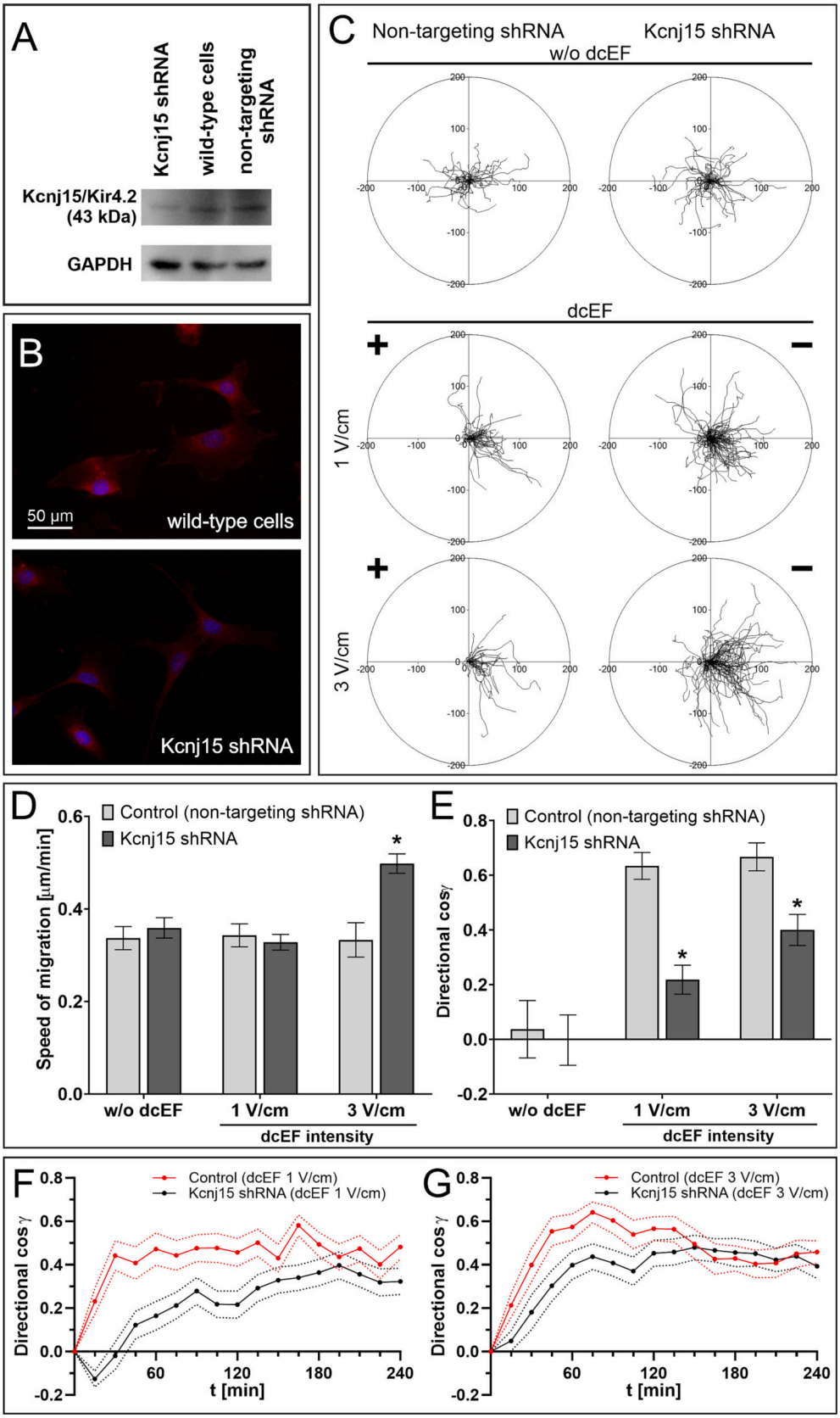

(caption on next page)

Fig. 9. The effect of Kcnj15 (Kir4.2 inwardly rectifying potassium channel) gene knockdown (with shRNA) on electrotaxis of 3T3 fibroblasts. (A) Western blot analysis showing a decreased level of Kir4.2 protein (product of Kcnj15 expression) in cells transduced with Kcnj15-shRNA compared to wild-type cells and transduced with nontargeting shRNA. (B) Immunocytofluorescence staining of Kir4.2 ion channels in cells (red) transduced with Kcnj15-shRNA compared to wild-type cells. Cell nuclei were counterstained with Hoechst 33258 (blue); the scale bar is common for both images. (C) Circular diagrams presenting composite cell trajectories under different conditions: 3T3 fibroblasts transduced with nontargeting shRNA as control conditions (w/o dcEF, and dcEF 1 V/cm or 3 V/cm) and cells transduced with Kcnj15-shRNA in corresponding conditions. Diagrams were constructed as previously described (see Fig. 1). (D) Speed of cell migration and (E) directionality of cell migration (presented as directional cos γ), calculated as the mean (for the analysed population) ± SEM. Cell numbers (*n*) are specified in Table 6. *Statistically significant differences relative to corresponding controls (cells transduced with nontargeting shRNA) ($p < 0.05$). (F, G) Dynamics of electrotaxis of cells transduced with Kcnj15 shRNA in a dcEF of 1 V/cm and 3 V/cm, respectively, compared to control conditions (wild-type cells), calculated as the mean directional cos γ ± SEM, with a 15-minute time interval. Cell numbers (*n*) are specified in Tables 1 and 6.

Table 6
The effect of Kcnj15 (Kir4.2 inwardly rectifying potassium channel) gene knockdown (with shRNA) on electrotaxis of 3T3 fibroblasts.

	Control (nontargeting shRNA)			Kcnj15 shRNA		
dcEF intensity	0 V/cm ($n = 40$)	1 V/cm ($n = 45$)	3 V/cm ($n = 33$)	0 V/cm ($n = 50$)	1 V/cm ($n = 103$)	3 V/cm ($n = 85$)
Speed of migration [μm/min]	0.337 ± 0.025	0.343 ± 0.025	0.333 ± 0.037	0.359 ± 0.022	0.328 ± 0.017	0.498 ± 0.021*
Displacement [μm]	44.492 ± 4.721	57.844 ± 5.662	52.280 ± 6.573	52.077 ± 4.693	51.603 ± 3.387	75.326 ± 4.469*
CME	0.549 ± 0.037	0.674 ± 0.032	0.675 ± 0.038	0.586 ± 0.034	0.624 ± 0.020	0.631 ± 0.023
Cosine γ	0.037 ± 0.105	0.634 ± 0.049	0.667 ± 0.051	−0.003 ± 0.092	0.218 ± 0.053*	0.400 ± 0.057*

* Statistically significant differences relative to corresponding controls (cells transduced with nontargeting shRNA) ($p < 0.05$).

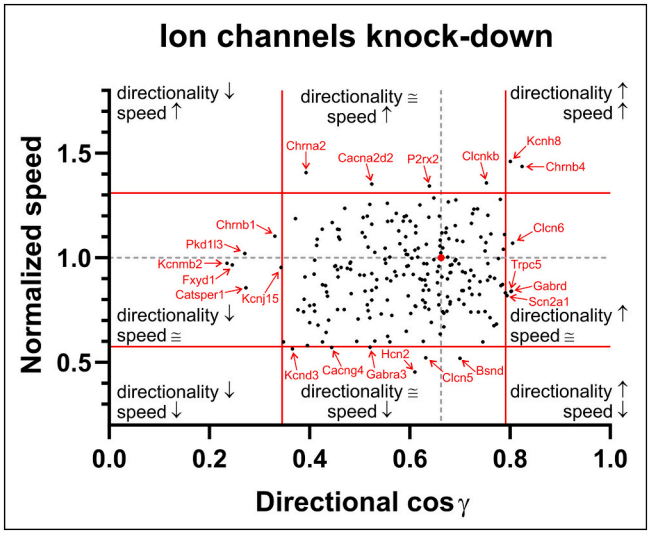

Fig. 10. The effect of silencing specific ion channel genes (with targeted siRNA) on the electrotaxis of 3T3 fibroblasts. The speed of cell migration (Y axis) is plotted against cell migration directionality (X axis). Each point represents one gene from the library ($n = 227$), presented as the mean for the analysed cell population ($n = 30$), migrating under 3 V/cm dcEF. The speed of cell migration was normalized to that of control cells (transfected with nontargeting siRNA) from the respective experiment. Control cells are represented by the red point, which is an average from 29 independent experiments. The directionality of cell migration is presented as directional cos γ. For both parameters, the 5 % most deviating conditions (2.5 % upper and lower cases) from the population average are separated with a red line, marked with an arrow, and described. The complete list of inhibited genes is provided in Supplementary Table A. Records in this table are ordered according to the value of the mean directional cosine γ and are accompanied by the corresponding value of normalized speed, both of which precisely indicate individual points within the plot. Conditions indicated by arrows in this figure are highlighted in red in the table, while the remaining points are described in black.

result may suggest that drawing conclusions about the participation of calcium ions in the electrotactic reaction only on the basis of experiments carried out in culture media devoid of calcium ions or in the presence of chelators may be misleading. This observation may also explain the previously mentioned discrepancies in the assessment of the role of calcium ions in electrotaxis [25,33,46,48].

In addition to calcium channels, several other ion channels have been suggested to be involved in the electrotactic reaction of various cell types [25,33,46,48]. Among others, voltage-gated Na^+ channels [7], voltage-gated potassium Kv1.2 channels [49], inwardly rectifying potassium channels (Kir4.2) [26] and ion transporters such as Na, K-ATPase (NaKA) and Na^+/H^+ exchanger isoforms (NHE1 and 3) [50]. In fact, inhibition of inwardly rectifying potassium channels (Kir4.2) significantly reduced the directional movement of 3T3 cells in dcEF. We demonstrated (Fig. 6) that Ba^{2+}, a broad-range blocker for a whole family of Kir channels [37], and specific inhibition of the expression of the Kcnj15 gene that encodes the Kir4.2 channel (Fig. 9) significantly reduce directional migration of 3T3 cells in dcEF. The responsibility of the Kcnj15/Kir4.2 channel for dcEF sensing by 3T3 fibroblasts was confirmed by investigating the effect of modification of the level of intracellular polyamines such as spermine (SPM) and spermidine (SPD) in 3T3 cells on their electrotaxis (Fig. 7). We demonstrated that changes in the level of those regulators of Kir family channels significantly affect the directionality of 3T3 cells in dcEF. Our observations in fibroblastic 3T3 cells are consistent with the results obtained by Nakajima et al. [26], who demonstrated the important role of Kir4.2 channels in the electrotaxis of epithelial cells. They showed that the knockdown of the KCNJ15 gene inhibits electrotaxis of those cells without affecting the speed of cell migration and that the depletion of cytoplasmic polyamines completely inhibited, whereas the increase in intracellular polyamines enhanced electrotaxis. We also confirmed the important role of Kir4.2 channels in the electrotaxis of 3T3 cells by applying a high concentration of Mg^{+2} ions (10 mM), which led to a clear decrease in the directionality of cell movement (Fig. 8, Table 5). As intracellular magnesium ions can be a factor regulating the activity of Kir 4.2 channels [51], we think that the high concentration of those ions in the cytoplasm may mask the effect of dcEF-induced asymmetrically redistributed polyamines and inhibit directional movement [26]. The results obtained indicate an important role for Kir4.2 channels in the electrotaxis of 3T3 cells. However, it is unlikely that this complex process is dependent solely on the activity of this channel. A large-scale screening method that we used to identify ion channel genes that are important in the electrotaxis of 3T3 cells revealed that many other ion channel genes (including K^+, Na^+, Ca^{2+} and Cl^- channels) may be involved in this process. This observation seems to be consistent with the data from the literature, which showed a significant share of different types of ion channels in different cell models [7,23,25,49,52,53]. However, there are still only a few reports on a comprehensive comparison of the effects of more

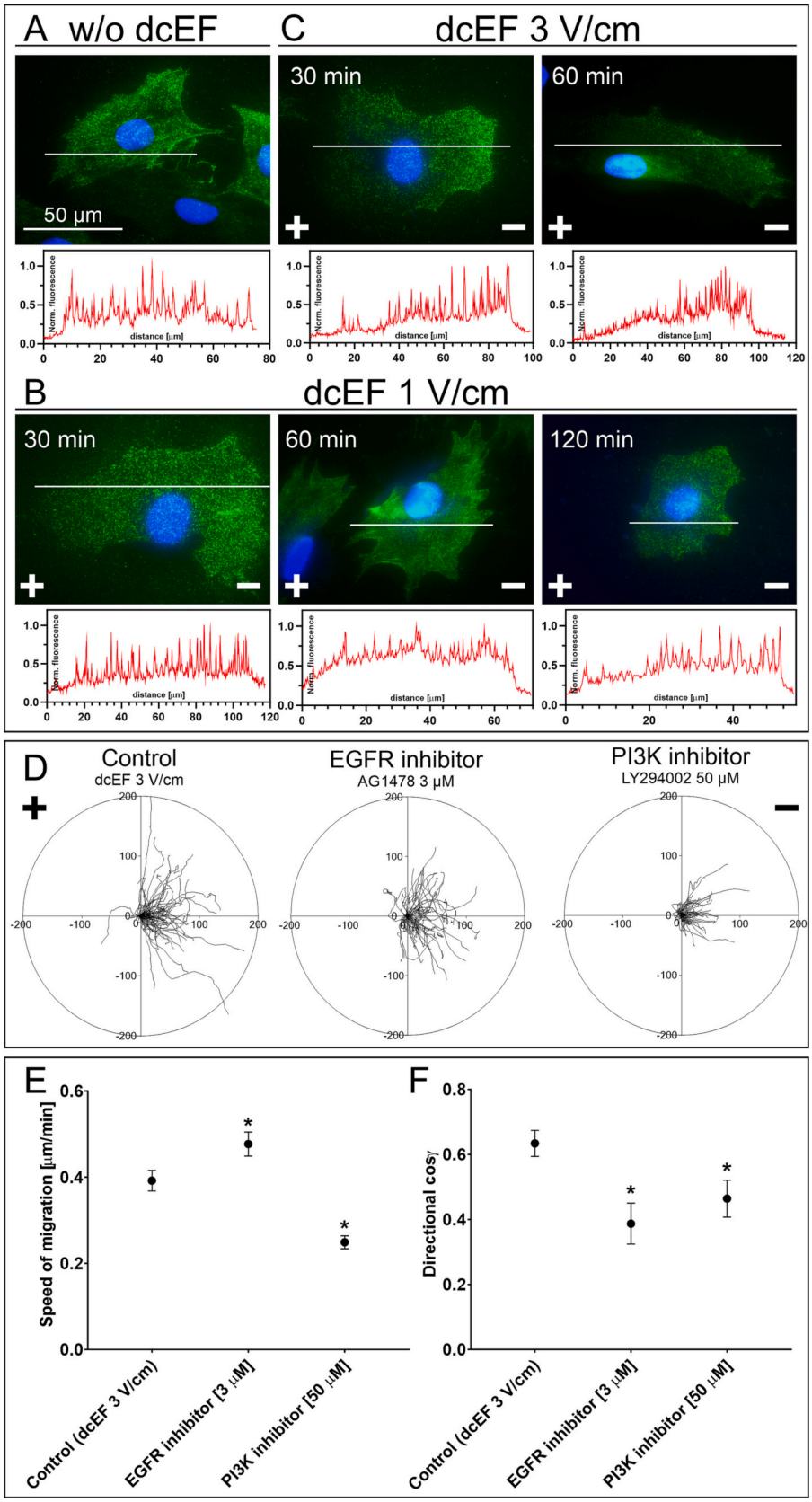

(caption on next page)

Fig. 11. The redistribution and role of EGFR in the electrotaxis of 3T3 fibroblasts. (A–C) Immunofluorescence staining of the EGF receptor (green) in cells without exposure to an electric field (A) and after a specified time of stimulation with dcEF 1 V/cm (B) or 3 V/cm (C). Images were captured with TIRF microscopy. Cell nuclei are counterstained with Hoechst 33258 (blue); the scale bar in (A) is common for all images. The cathode of the dcEF (if present) is located on the right side of the field of view. Each image is accompanied by a corresponding plot profile, presenting normalized green fluorescence intensity measured along the white line. (D) Circular diagrams presenting composite cell trajectories under control conditions (dcEF 3 V/cm) or in culture medium with EGFR and PI3K inhibitors (AG1478 3 μM and LY294002 50 μM, respectively). Diagrams were constructed as previously described (see Fig. 1). (E) Speed of cell migration and (F) directionality of cell migration (presented as directional cos γ), calculated as the mean (for the analysed population) ± SEM. The number of cells (*n*) analysed for each condition was 70, 50, and 50, respectively. *Statistically significant differences relative to control ($p < 0.05$).

channel types in one cellular model [26]. These observations indicate that the cell's response to an electric field may be due to the interaction of multiple types of ion channels. However, it is still not clear which of these channels are directly activated by the external electric field during electrotaxis and what is the mechanism of their activation.

Our results suggest that the primary reaction of 3T3 cells to dcEF is related to the activation of specific ion channels rather than the translocation of receptors in the plasma membrane. However, the role of the redistribution of chemoattractant receptors on the cell membrane in electrotaxis is very well documented. For example, the EGF receptor has been suggested to play a critical role in the electrotactic response of corneal epithelial cells, keratinocytes and breast cancer cells [39,40,54]. The application of small dcEFs upregulates the expression of EGF receptors and induces an asymmetrical distribution of EGF receptors. When keratinocytes are placed in dcEF in vitro, EGF receptors become more concentrated on the side of the cell facing the cathode. Moreover, corneal epithelial cells (CECs), which migrate cathodally in FCS-containing media, in serum-free medium lose all directionality in the dcEF (although they continue to migrate). Adding EGF (but also bFGF or TGB-β1) restores directed migration. This suggests that several growth factor receptors may act together, perhaps using a parallel signalling pathway, to transduce the effects of a dcEF. In recent years, this hypothesis has been confirmed in several other models, and several membrane receptors, such as the epidermal growth factor receptor (EGFR), concanavalin A receptor (ConA), sodium-hydrogen exchanger 3 (pNHE3), *N*-methyl-D-aspartate receptor (NMDAR), acetylocholine receptor (AchR), or integrins, were shown to be redistributed under the influence of dcEF and involved in cell electrotaxis [39,40,50,55–59]. However, both mechanisms are in fact not mutually exclusive. Mycielska and Djamgoz [19] suggested that cells migrating in the electric field have both short-term and long-term responses and that translocation of cell membrane receptors is important only for long-term reactions. Our finding that inhibition of the Kir4.2 channel abolishes the directional movement of 3T3 cells in dcEF for only approximately 1–2 h and then the reappearance of electrotaxis can be observed confirms the validity of this hypothesis. Therefore, we suggest here the biphasic mechanism of electrotaxis, the complementary role of ion channels, and chemoattractant receptors in this process. We hypothesize that the ionic mechanism of electrotaxis is responsible for the first very fast cell reaction, but after a sufficiently long time (a time scale of a dozen minutes), the redistribution of receptors on the cell membrane may be sufficiently clear to be responsible for directing cell migration in the electric field. However, this hypothesis requires further research because another possible explanation is that after prolonged exposure to the electric field, the lack of Kcnj15 channel activity may be compensated by other ion channels.

In summary, we have shown that even in slowly migrating 3T3 cells, the reaction to dcEF is relatively fast, with the first symptoms visible after 1 min of exposure to dcEF. This strongly suggests that the primary mechanism of the electrotactic reaction is related to the activation of ion channels rather than to the translocation of cell membrane receptors. Indeed, a large-scale screening method that we used to identify ion channel genes that are important in 3T3 electrotaxis revealed that several ion channel genes may be involved in this process. Among others, the electrotactic reaction of 3T3 cells strongly depended on inwardly rectifying potassium channels (Kir4.2). As the inhibition of the Kir4.2 channel reduces the directional movement of 3T3 cells for only approximately 1–2 h and then the reappearance of electrotaxis can be observed, we suggest a biphasic mechanism of electrotaxis of mouse 3T3 fibroblasts, in which the activation of ion channels is responsible for the first quick reaction of the cell to an electric field and the redistribution of membrane receptors for long-term maintenance of the direction of cell movement.

Supplementary Movies: Migration of 3T3 fibroblasts: (A) under isotropic conditions, (B) under a dcEF of 1 V/cm, and (C) 3 V/cm. Images captured every 30 s for 4 h and 30 min with dcEF applied (if present) after the initial 30 min. The movie frame rate is 40 fps. (D) Dynamics of the response to a 3 V/cm dcEF reversal. Images captured every 60 s for 4 h with the cathode located at the right side of the field of view until 120 min, and transferred to the left side for subsequent 120 min. Frame rate 20 fps. (E) 3T3 fibroblasts after knockdown of Kcnj15/Kir.4.2 migrating in a dcEF of 1 V/cm. Movie parameters as described previously (A-C). The scale bar is equal to 100 μm at each movie. Supplementary data to this article can be found online at https://doi.org/10.1016/j.bbamcr.2023.119647.

Funding

This work was supported by a grant from the National Science Centre 2018/31/B/NZ3/01750, Poland.

CRediT authorship contribution statement

Slawomir Lasota: Conceptualization, Data curation, Formal analysis, Funding acquisition, Investigation, Methodology, Project administration, Software, Validation, Visualization, Writing – original draft, Writing – review & editing. **Eliza Zimolag:** Methodology. **Sylwia Bobis-Wozowicz:** Investigation, Methodology, Resources. **Jagoda Pilipiuk:** Investigation. **Zbigniew Madeja:** Conceptualization, Data curation, Funding acquisition, Methodology, Project administration, Resources, Supervision, Validation, Writing – original draft, Writing – review & editing.

Declaration of competing interest

The authors declare that they have no known competing financial interests or personal relationships that could have appeared to influence the work reported in this paper.

Data availability

Data will be made available on request.

References

[1] S. SenGupta, C.A. Parent, J.E. Bear, The principles of directed cell migration, Nat. Rev. Mol. Cell Biol. 22 (2021) 529–547, https://doi.org/10.1038/s41580-021-00366-6.
[2] D.S. Pal, X. Li, T. Banerjee, Y. Miao, P.N. Devreotes, The excitable signal transduction networks: movers and shapers of eukaryotic cell migration, Int. J. Dev. Biol. 63 (2019) 407–416, https://doi.org/10.1387/ijdb.190265pd.
[3] P.A. Iglesias, P.N. Devreotes, Biased excitable networks: how cells direct motion in response to gradients, Curr. Opin. Cell Biol. 24 (2012) 245–253, https://doi.org/10.1016/j.ceb.2011.11.009.
[4] Y. Artemenko, T.J. Lampert, P.N. Devreotes, Moving towards a paradigm: common mechanisms of chemotactic signaling in Dictyostelium and mammalian leukocytes,

Cell. Mol. Life Sci. 71 (2014) 3711–3747, https://doi.org/10.1007/s00018-014-1638-8.
[5] B. Wójciak-Stothard, Z. Madeja, W. Korohoda, A. Curtis, C. Wilkinson, Activation of macrophage-like cells by multiple grooved substrata. Topographical control of cell behaviour, Cell Biol. Int. 19 (1995) 485–490, https://doi.org/10.1006/cbir.1995.1092.
[6] W. Korohoda, M. Mycielska, E. Janda, Z. Madeja, Immediate and long-term galvanotactic responses of *Amoeba proteus* to dc electric fields, Cell Motil. Cytoskeleton 45 (2000) 10–26, https://doi.org/10.1002/(SICI)1097-0169(200001)45:1<10::AID-CM2>3.0.CO;2-T.
[7] M.B.A. Djamgoz, M. Mycielska, Z. Madeja, S.P. Fraser, W. Korohoda, Directional movement of rat prostate cancer cells in direct-current electric field: involvement of voltagegated Na^+ channel activity, J. Cell Sci. 114 (2001) 2697–2705, https://doi.org/10.1242/jcs.114.14.2697.
[8] W. Korohoda, Z. Madeja, J. Sroka, Diverse chemotactic responses of *Dictyostelium discoideum* amoebae in the developing (temporal) and stationary (spatial) concentration gradients of folic acid, cAMP, Ca(2+) and Mg(2+), Cell Motil. Cytoskeleton 53 (2002) 1–25, https://doi.org/10.1002/cm.10052.
[9] C.D. McCaig, A.M. Rajnicek, B. Song, M. Zhao, Controlling cell behavior electrically: current views and future potential, Physiol. Rev. 85 (2005) 943–978, https://doi.org/10.1152/physrev.00020.2004.
[10] C.D. McCaig, B. Song, A.M. Rajnicek, Electrical dimensions in cell science, J. Cell Sci. 122 (2009) 4267–4276, https://doi.org/10.1242/jcs.023564.
[11] A.T. Barker, L.F. Jaffe, J.W. Vanable, The glabrous epidermis of cavies contains a powerful battery, Am. J. Phys. 242 (1982) R358–R366, https://doi.org/10.1152/ajpregu.1982.242.3.R358.
[12] D.D. Sta Iglesia, J.W. Vanable, Endogenous lateral electric fields around bovine corneal lesions are necessary for and can enhance normal rates of wound healing, Wound Repair Regen. 6 (1998) 531–542, https://doi.org/10.1046/j.1524-475x.1998.60606.x.
[13] B. Reid, R. Nuccitelli, M. Zhao, Non-invasive measurement of bioelectric currents with a vibrating probe, Nat. Protoc. 2 (2007) 661–669, https://doi.org/10.1038/nprot.2007.91.
[14] M. Zhao, Electrical fields in wound healing-an overriding signal that directs cell migration, Semin. Cell Dev. Biol. 20 (2009) 674–682, https://doi.org/10.1016/j.semcdb.2008.12.009.
[15] G.M. Allen, A. Mogilner, J.A. Theriot, Electrophoresis of cellular membrane components creates the directional cue guiding keratocyte galvanotaxis, Curr. Biol. 23 (2013) 560–568, https://doi.org/10.1016/j.cub.2013.02.047.
[16] L.F. Jaffe, Electrophoresis along cell membranes, Nature 265 (1977) 600–602, https://doi.org/10.1038/265600a0.
[17] M. Zhao, A. Dick, J.V. Forrester, C.D. McCaig, Electric field-directed cell motility involves up-regulated expression and asymmetric redistribution of the epidermal growth factor receptors and is enhanced by fibronectin and laminin, Mol. Biol. Cell 10 (1999) 1259–1276, https://doi.org/10.1091/mbc.10.4.1259.
[18] A. Sarkar, B.M. Kobylkevich, D.M. Graham, M.A. Messerli, Electromigration of cell surface macromolecules in DC electric fields during cell polarization and galvanotaxis, J. Theor. Biol. 478 (2019) 58–73, https://doi.org/10.1016/j.jtbi.2019.06.015.
[19] M.E. Mycielska, M.B.A. Djamgoz, Cellular mechanisms of direct-current electric field effects: galvanotaxis and metastatic disease, J. Cell Sci. 117 (2004) 1631–1639, https://doi.org/10.1242/jcs.01125.
[20] R.-C. Chi Gao, X.-D. Dong Zhang, Y.-H. Hui Sun, Y. Kamimura, A. Mogilner, P. N. Devreotes, M. Zhao, Different roles of membrane potentials in electrotaxis and chemotaxis of dictyostelium cells, Eukaryot. Cell 10 (2011) 1251–1256, https://doi.org/10.1128/EC.05066-11.
[21] J. Sroka, I. Krecioch, E. Zimolag, S. Lasota, M. Rak, S. Kedracka-Krok, P. Borowicz, M. Gajek, Z. Madeja, Lamellipodia and membrane blebs drive efficient electrotactic migration of rat Walker carcinosarcoma cells WC 256, PLoS One 11 (2016), e0149133, https://doi.org/10.1371/journal.pone.0149133.
[22] E. Zimolag, J. Borowczyk-Michalowska, S. Kedracka-Krok, B. Skupien-Rabian, E. Karnas, S. Lasota, J. Sroka, J. Drukala, Z. Madeja, Electric field as a potential directional cue in homing of bone marrow-derived mesenchymal stem cells to cutaneous wounds, Biochim. Biophys. Acta (BBA) - Mol. Cell Res. 1864 (2017) 267–279, https://doi.org/10.1016/j.bbamcr.2016.11.011.
[23] D.R. Trollinger, R.R. Isseroff, R. Nuccitelli, Calcium channel blockers inhibit galvanotaxis in human keratinocytes, J. Cell. Physiol. 193 (2002) 1–9, https://doi.org/10.1002/jcp.10144.
[24] D.M. Graham, L. Huang, K.R. Robinson, M.A. Messerli, Epidermal keratinocyte polarity and motility require Ca^{2+} influx through TRPV1, J. Cell Sci. 126 (2013) 4602–4613, https://doi.org/10.1242/jcs.122192.
[25] L. Guo, C. Xu, D. Li, X. Zheng, J. Tang, J. Bu, H. Sun, Z. Yang, W. Sun, X. Yu, Calcium ion flow permeates cells through SOCs to promote cathode-directed galvanotaxis, PLoS One 10 (2015), e0139865, https://doi.org/10.1371/journal.pone.0139865.
[26] K. Nakajima, K. Zhu, Y.-H. Sun, B. Hegyi, Q. Zeng, C.J. Murphy, J.V. Small, Y. Chen-Izu, Y. Izumiya, J.M. Penninger, M. Zhao, KCNJ15/Kir4.2 couples with polyamines to sense weak extracellular electric fields in galvanotaxis, Nat. Commun. 6 (2015) 8532, https://doi.org/10.1038/ncomms9532.
[27] J. Sroka, E. Zimolag, S. Lasota, W. Korohoda, Z. Madeja, Electrotaxis: cell directional movement in electric fields, in: Methods in Molecular Biology, 2018, pp. 325–340, https://doi.org/10.1007/978-1-4939-7701-7_23.
[28] J. Schindelin, I. Arganda-Carreras, E. Frise, V. Kaynig, M. Longair, T. Pietzsch, S. Preibisch, C. Rueden, S. Saalfeld, B. Schmid, J.Y. Tinevez, D.J. White, V. Hartenstein, K. Eliceiri, P. Tomancak, A. Cardona, Fiji: an open-source platform for biological-image analysis, Nat. Methods 9 (2012) 676–682, https://doi.org/10.1038/NMETH.2019.
[29] I. Krecioch, Z. Madeja, S. Lasota, E. Zimolag, J. Sroka, The role of microtubules in electrotaxis of rat Walker carcinosarcoma WC256 cells, Acta Biochim. Pol. 62 (2015) 401–406, https://doi.org/10.18388/abp.2015_1019.
[30] M. Michalik, E. Soczek, M. Kosińska, M. Rak, K.A. Wójcik, S. Lasota, M. Pierzchalska, J. Czyż, Z. Madeja, Lovastatin-induced decrease of intracellular cholesterol level attenuates fibroblast-to-myofibroblast transition in bronchial fibroblasts derived from asthmatic patients, Eur. J. Pharmacol. 704 (2013) 23–32, https://doi.org/10.1016/j.ejphar.2013.02.023.
[31] N. Orida, J.D. Feldman, Directional protrusive pseudopodial activity and motility in macrophages induced by extracellular electric fields, Cell Motil. 2 (1982) 243–255, https://doi.org/10.1002/cm.970020305.
[32] M.S. Cooper, M. Schliwa, Electrical and ionic controls of tissue cell locomotion in DC electric fields, J. Neurosci. Res. 13 (1985) 223–244, https://doi.org/10.1002/jnr.490130116.
[33] E.K. Onuma, S.W. Hui, Electric field-directed cell shape changes, displacement, and cytoskeletal reorganization are calcium dependent, J. Cell Biol. 106 (1988) 2067–2075, https://doi.org/10.1083/jcb.106.6.2067.
[34] L.J. Shanley, P. Walczysko, M. Bain, D.J. MacEwan, M. Zhao, Influx of extracellular Ca^{2+} is necessary for electrotaxis in Dictyostelium, J. Cell Sci. 119 (2006) 4741–4748, https://doi.org/10.1242/jcs.03248.
[35] E.K. Onuma, S.W. Hui, A calcium requirement for electric field-induced cell shape changes and preferential orientation, Cell Calcium 6 (1985) 281–292, https://doi.org/10.1016/0143-4160(85)90012-0.
[36] G.W. deHart, T. Jin, D.E. McCloskey, A.E. Pegg, D. Sheppard, The alpha9beta1 integrin enhances cell migration by polyamine-mediated modulation of an inward-rectifier potassium channel, Proc. Natl. Acad. Sci. U. S. A. 105 (2008) 7188–7193, https://doi.org/10.1073/pnas.0708044105.
[37] J.M. Quayle, J.G. McCarron, J.E. Brayden, M.T. Nelson, Inward rectifier K+ currents in smooth muscle cells from rat resistance-sized cerebral arteries, Am. J. Phys. 265 (1993) C1363–C1370, https://doi.org/10.1152/ajpcell.1993.265.5.C1363.
[38] V.A. Baronas, H.T. Kurata, Inward rectifiers and their regulation by endogenous polyamines, Front. Physiol. 5 (2014) 325, https://doi.org/10.3389/fphys.2014.00325.
[39] M. Zhao, J. Pu, J.V. Forrester, C.D. McCaig, Membrane lipids, EGF receptors, and intracellular signals colocalize and are polarized in epithelial cells moving directionally in a physiological electric field, FASEB J. 16 (2002) 857–859, https://doi.org/10.1096/fj.01-0811fje.
[40] K.S. Fang, E. Ionides, G. Oster, R. Nuccitelli, R.R. Isseroff, Epidermal growth factor receptor relocalization and kinase activity are necessary for directional migration of keratinocytes in DC electric fields, J. Cell Sci. 112 (Pt 12) (1999) 1967–1978, https://doi.org/10.1242/jcs.112.12.1967.
[41] F.X. Hart, M. Laird, A. Riding, C.E. Pullar, Keratinocyte galvanotaxis in combined DC and AC electric fields supports an electromechanical transduction sensing mechanism, Bioelectromagnetics 34 (2013) 85–94, https://doi.org/10.1002/bem.21748.
[42] W.P. Yang, E.K. Onuma, S.W. Hui, Response of C3H/10T1/2 fibroblasts to an external steady electric field stimulation. Reorientation, shape change, ConA receptor and intramembranous particle distribution and cytoskeleton reorganization, Exp. Cell Res. 155 (1984) 92–104, https://doi.org/10.1016/0014-4827(84)90770-5.
[43] S. McLaughlin, M.M. Poo, The role of electro-osmosis in the electric-field-induced movement of charged macromolecules on the surfaces of cells, Biophys. J. 34 (1981) 85–93, https://doi.org/10.1016/S0006-3495(81)84838-2.
[44] D.W. Tank, W.J. Fredericks, L.S. Barak, W.W. Webb, Electric field-induced redistribution and postfield relaxation of low density lipoprotein receptors on cultured human fibroblasts, J. Cell Biol. 101 (1985) 148–157, https://doi.org/10.1083/jcb.101.1.148.
[45] S. Lin-Liu, W.R. Adey, M.M. Poo, Migration of cell surface concanavalin A receptors in pulsed electric fields, Biophys. J. 45 (1984) 1211–1217, https://doi.org/10.1016/S0006-3495(84)84270-8.
[46] M.J. Brown, L.M. Loew, Electric field-directed fibroblast locomotion involves cell surface molecular reorganization and is calcium independent, J. Cell Biol. 127 (1994) 117–128, https://doi.org/10.1083/jcb.127.1.117.
[47] R. Nuccitelli, T. Smart, Extracellular calcium levels strongly influence neural crest cell galvanotaxis, Biol. Bull. 176 (1989) 130–135, https://doi.org/10.2307/1541662.
[48] S.M. Ross, J.M. Ferrier, J.E. Aubin, Studies on the alignment of fibroblasts in uniform applied electrical fields, Bioelectromagnetics 10 (1989) 371–384, https://doi.org/10.1002/bem.2250100406.
[49] G. Zhang, M. Edmundson, V. Telezhkin, Y. Gu, X. Wei, P.J. Kemp, B. Song, The role of Kv1.2 channel in electrotaxis cell migration, J. Cell. Physiol. 231 (2016) 1375–1384, https://doi.org/10.1002/jcp.25259.
[50] N. Özkucur, S. Perike, P. Sharma, R.H.W. Funk, Persistent directional cell migration requires ion transport proteins as direction sensors and membrane potential differences in order to maintain directedness, BMC Cell Biol. 12 (2011) 4, https://doi.org/10.1186/1471-2121-12-4.
[51] Z. Lu, Mechanism of rectification in inward-rectifier K^+ channels, Annu. Rev. Physiol. 66 (2004) 103–129, https://doi.org/10.1146/annurev.physiol.66.032102.150822.
[52] H.-F. Tsai, C. IJspeert, A.Q. Shen, Voltage-gated ion channels mediate the electrotaxis of glioblastoma cells in a hybrid PMMA/PDMS microdevice, APL Bioeng. 4 (2020), 036102, https://doi.org/10.1063/5.0004893.

[53] Y. Li, W.-K. Yu, L. Chen, Y.-S. Chan, D. Liu, C.-C. Fong, T. Xu, G. Zhu, D. Sun, M. Yang, Electrotaxis of tumor-initiating cells of H1975 lung adenocarcinoma cells is associated with both activation of stretch-activated cation channels (SACCs) and internal calcium release, Bioelectrochemistry 124 (2018) 80–92, https://doi.org/10.1016/j.bioelechem.2018.03.013.

[54] J. Pu, C.D. McCaig, L. Cao, Z. Zhao, J.E. Segall, M. Zhao, EGF receptor signalling is essential for electric-field-directed migration of breast cancer cells, J. Cell Sci. 120 (2007) 3395–3403, https://doi.org/10.1242/jcs.002774.

[55] L. Huang, P. Cormie, M.A. Messerli, K.R. Robinson, The involvement of Ca^{2+} and integrins in directional responses of zebrafish keratocytes to electric fields, J. Cell. Physiol. 219 (2009) 162–172, https://doi.org/10.1002/jcp.21660.

[56] L. Li, Y.H. El-Hayek, B. Liu, Y. Chen, E. Gomez, X. Wu, K. Ning, L. Li, N. Chang, L. Zhang, Z. Wang, X. Hu, Q. Wan, Direct-current electrical field guides neuronal stem/progenitor cell migration, Stem Cells 26 (2008) 2193–2200, https://doi.org/10.1634/stemcells.2007-1022.

[57] N. Orida, M.M. Poo, Electrophoretic movement and localisation of acetylcholine receptors in the embryonic muscle cell membrane, Nature 275 (1978) 31–35, https://doi.org/10.1038/275031a0.

[58] M. Poo, K.R. Robinson, Electrophoresis of concanavalin A receptors along embryonic muscle cell membrane, Nature 265 (1977) 602–605, https://doi.org/10.1038/265602a0.

[59] C.E. Pullar, B.S. Baier, Y. Kariya, A.J. Russell, B.A.J. Horst, M.P. Marinkovich, R. R. Isseroff, beta4 integrin and epidermal growth factor coordinately regulate electric field-mediated directional migration via Rac1, Mol. Biol. Cell 17 (2006) 4925–4935, https://doi.org/10.1091/mbc.e06-05-0433.